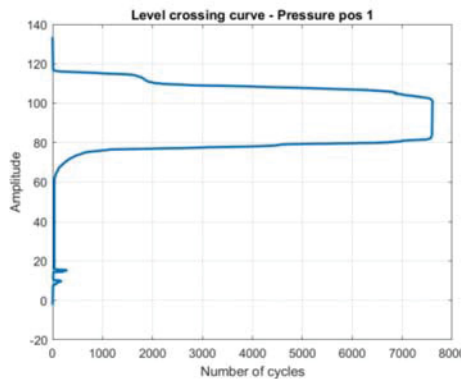


# Development of Tool in MATLAB for the Durability Prediction of Radiators



**Akhil Mora**  
**Raghavendra Machipeddi**

Department of Mechanical Engineering  
Blekinge Institute of Technology  
Karlskrona, Sweden

2017



# **Development of Tool in MATLAB for the Durability Prediction of Radiators**

**Akhil Mora  
Raghavendra Machipeddi**

Department of Mechanical Engineering

Blekinge Institute of Technology

Karlskrona, Sweden

2017

Thesis submitted for completion of Master of Science in Mechanical Engineering with emphasis on Structural Mechanics at the department of Mechanical Engineering, Blekinge Institute of Technology, Karlskrona, Sweden.

**Abstract:**

Durability is the most important factor in the design of heat-exchangers to meet the specifications of the customers. To predict the durability, endurance tests are carried out. In this thesis, one of the endurance tests, thermal cycling is performed for three different internal coolant flows until failure which is known as Wöhler test. A tool is developed in MATLAB that could import data from all kinds of endurance tests and visualizes time histories of every channel of the test (test parameters such as temperature, pressure, flow). An algorithm is developed for Level Crossing counting method which works based on the Markov cycle counting method. This produces Level crossing curves (LCC) for all the channels of the test which says how well a test has been performed and the total number of cycles of the test. It was observed that the LCCs obtained from the tool gives accurate results when compared with those obtained from LMS software whose approach of producing LCCs is Rainflow cycle counting method. Strain measurements are performed for the same flowrates as that of the Wöhler tests. The results from strain measurements and Wöhler tests are used in the determination of Basquin's coefficient of the Wöhler curve. It was observed that the optimal value of Basquin's coefficient is 3.4.

**Keywords:**

Basquin's coefficient, Cycle counting, Level Crossing, Thermal Cycling, Wöhler curve.

# Acknowledgements

This work was carried out at the Department of Mechanical Engineering, Blekinge Institute of Technology (BTH), Karlskrona, Sweden and TitanX Engine Cooling AB, Mjällby, Sweden from January 2017 to October 2017 under the supervision of Dr. Ansel Berghuvud, and Tobias Karlsson.

First and foremost, we would like to thank our parents for their endless love and support over the years.

We wish to express our sincere gratitude to our main promoter Anders Brorsson, RD&E Director OU ESA, our industrial supervisor Tobias Karlsson and Magnus Nilsson, Test Center Manager, for their guidance and professional engagement throughout the work.

We want to express our deep gratitude to our academic supervisor Dr. Ansel Berghuvud for his guidance, valuable suggestions and support.

We would also like to express our gratitude to our friend, Rohan Appilla Chakravarthula, Developer, Ericsson, who helped us in difficult situations in the coding part of MATLAB.

Karlskrona, October 2017

*Akhil Mora*

*Raghavendra Machipeddi*

# Contents

<b>List of figures</b>	<b>6</b>
<b>List of Tables</b>	<b>8</b>
<b>1 Notations</b>	<b>9</b>
<b>2 Introduction</b>	<b>11</b>
2.1 Background	11
2.2 Problem description	12
2.3 Aim and objectives	12
2.4 Research Questions	13
2.5 Delimitations	14
2.6 Disposition	14
<b>3 Related work</b>	<b>15</b>
3.1 Literature study	15
3.1.1 Strain gauges	15
3.1.2 Cycle counting methods	21
<b>4 Studied system</b>	<b>24</b>
4.1 Material data and Material Model	25
<b>5 Overview of the Method</b>	<b>26</b>
<b>6 Experimentation process</b>	<b>27</b>
6.1 Strain Measurements	27
6.2 Wöhler Testing	32
6.3 Results from experimentation	33
6.3.1 Strain measurements	33
6.3.2 Wöhler testing	35
<b>7 Development of tool</b>	<b>41</b>
7.1 Data importing	41
7.2 Level Crossing Cycle Counting	44
7.2.1 Implementation of Level Crossing Cycle Counting	44
7.2.2 Real data from test bench	48
7.2.3 Level Crossing counting for Real data	52
7.3 Graphical user interface (GUI)	54
<b>8 Investigation of Basquin's Coefficient</b>	<b>55</b>
<b>9 Results</b>	<b>61</b>
<b>10 Summary and Conclusions</b>	<b>64</b>

<b>11 Future works</b>	<b>65</b>
<b>12 References</b>	<b>66</b>
<b>13 Appendix</b>	<b>67</b>
A. Numbering of tubes on radiator	67
B. Level crossing curves from Wöhler Testing	67

# List of figures

<i>Figure 2.1. A typical radiator.</i> .....	11
<i>Figure 3.1. A foil strain gauge.</i> .....	16
<i>Figure 3.2. Gauge nomenclature [2].</i> .....	16
<i>Figure 3.3. Wheatstone bridge.</i> .....	17
<i>Figure 3.4. Wheatstone bridge with Shunt resistor.</i> .....	18
<i>Figure 3.5. Two-wire quarter-bridge circuit.</i> .....	19
<i>Figure 3.6. Three-wire quarter-bridge circuit.</i> .....	19
<i>Figure 3.7. Half-bridge circuit.</i> .....	20
<i>Figure 3.8. Full-bridge circuit.</i> .....	20
<i>Figure 4.1. Studied Radiator.</i> .....	24
<i>Figure 4.2. Thermal cycling Test Bench.</i> .....	25
<i>Figure 5.1. Method overview.</i> .....	26
<i>Figure 6.1. Kyowa Strain gauge.</i> .....	28
<i>Figure 6.2. Strain gauges installed on Radiator.</i> .....	29
<i>Figure 6.3. Strain gauges with the solder terminal and bridge circuit.</i> .....	30
<i>Figure 6.4. Bridge with Shunt resistance.</i> .....	31
<i>Figure 6.5. Two radiators mounted in the test bench.</i> .....	32
<i>Figure 6.6. Radiator with cut breakaways.</i> .....	33
<i>Figure 6.7. Strain Range.</i> .....	35
<i>Figure 6.8. Failure positions of object 1.</i> .....	36
<i>Figure 6.9. Failure position of object 2.</i> .....	36
<i>Figure 6.10. Failure position of object 4.</i> .....	37
<i>Figure 6.11. Failure position of object 5.</i> .....	38
<i>Figure 6.12. Failure position of object 6.</i> .....	38
<i>Figure 6.13. Failure position compared with thermographic image of object 5.</i> .....	39
<i>Figure 6.14. Failure position compared with thermographic image of object 6.</i> .....	40
<i>Figure 7.1. Synthetic signal 1.</i> .....	45
<i>Figure 7.2. Level crossing curve for synthetic signal 1 from MATLAB.</i> ....	46
<i>Figure 7.3. Level crossing curve for synthetic signal 1 from LMS.</i> .....	46
<i>Figure 7.4. Synthetic signal 2.</i> .....	47
<i>Figure 7.5. Level crossing curve for synthetic signal 2 from MATLAB.</i> ....	47
<i>Figure 7.6. Level crossing curve of synthetic signal 2 from LMS.</i> .....	48

<i>Figure 7.7. Time history of temperature (1 day).</i> .....	49
<i>Figure 7.8. Time history of pressure (1 day).</i> .....	49
<i>Figure 7.9. Time history of flow (1 day).</i> .....	50
<i>Figure 7.10. Time history of temperature (5 cycles).</i> .....	50
<i>Figure 7.11. Time history of pressure (5 cycles).</i> .....	51
<i>Figure 7.12. Time history of flow (5 cycles).</i> .....	51
<i>Figure 7.13. Level crossing curve of Temperature history.</i> .....	52
<i>Figure 7.14. Level crossing curve of Pressure history.</i> .....	53
<i>Figure 7.15. Level crossing curve of Flow history.</i> .....	53
<i>Figure 7.16. GUI of tool developed.</i> .....	54
<i>Figure 8.1. Wöhler curve (log-log scale).</i> .....	58
<i>Figure 8.2. Wöhler curve (semi-log scale).</i> .....	59
<i>Figure 9.1. Temperature history of one day data.</i> .....	62
<i>Figure 9.2. Level crossing spectrum of Temperature data for one day.</i> .....	62
<i>Figure 13.1. Engine side (Tubes 1-88).</i> .....	67
<i>Figure 13.2. LCC of Inlet and Outlet Temperature (Object 1).</i> .....	68
<i>Figure 13.3. LCC of Pressure (Object 1).</i> .....	68
<i>Figure 13.4. LCC of Flow (Object 1).</i> .....	68
<i>Figure 13.5. LCC of Inlet and Outlet Temperature (Object 2).</i> .....	69
<i>Figure 13.6. LCC of Pressure (Object 2).</i> .....	69
<i>Figure 13.7. LCC of Flow (Object 2).</i> .....	69
<i>Figure 13.8. LCC of Inlet and Outlet Temperature (Object 3).</i> .....	70
<i>Figure 13.9. LCC of Pressure (Object 3).</i> .....	70
<i>Figure 13.10. LCC of Flow (Object 3).</i> .....	70
<i>Figure 13.11. LCC of Inlet and Outlet Temperature (Object 4).</i> .....	71
<i>Figure 13.12. LCC of Pressure (Object 4).</i> .....	71
<i>Figure 13.13. LCC of Flow (Object 4).</i> .....	71
<i>Figure 13.14. LCC of Inlet and Outlet Temperature (Object 5).</i> .....	72
<i>Figure 13.15. LCC of Pressure (Object 5).</i> .....	72
<i>Figure 13.16. LCC of Flow (Object 5).</i> .....	72
<i>Figure 13.17. LCC of Inlet and Outlet Temperature (Object 6).</i> .....	73
<i>Figure 13.18. LCC of Pressure (Object 6).</i> .....	73
<i>Figure 13.19. LCC of Flow (Object 6).</i> .....	73

# List of Tables

<i>Table 4.1. Material properties of Aluminum.....</i>	25
<i>Table 6.1. Gauge dimensions.....</i>	28
<i>Table 6.2. Position of strain gauges. ....</i>	29
<i>Table 6.3. Channel set-up analysis. ....</i>	31
<i>Table 6.4. Maximum strain range.....</i>	34
<i>Table 6.5. Cycles to failure of each object.....</i>	39
<i>Table 7.1. Sample data from day 1. ....</i>	42
<i>Table 7.2. Sample data from day 2. ....</i>	42
<i>Table 7.3. Concatenated data of the whole test. ....</i>	43
<i>Table 8.1. Wöhler results. ....</i>	55
<i>Table 8.2. Stress and strain values for each flow. ....</i>	56

# 1 Notations

E	Young's Modulus
N	Number of cycles
$R_0$	Unstrained Gauge Resistance
$R_2$	Resistance in Wheatstone bridge
$R_3$	Resistance in Wheatstone bridge
$R_4$	Resistance in Wheatstone bridge
$R_L$	Lead wire resistance
$R_S$	Shunt resistance
$R_x$	Unknown resistance in Wheatstone bridge
$\Delta R$	Change in resistance in the gauge
S	Stress (Basquin's relation)
$\alpha$	Constant based on material (Basquin's relation)
$\beta$	Basquin's coefficient
$\varepsilon$	Strain
$\sigma$	Stress

## **Abbreviations**

GF	Gauge Factor (Strain gauge)
GUI	Graphical User Interface
LCC	Level crossing curve
TP	Turning points

## 2 Introduction

TitanX Engine Cooling AB in Mjällby is the leading global company that develops and manufactures heat-exchangers. Before introducing a new product into the market, different kinds of tests are carried out such as corrosion, vibration, pressure pulsation and thermal cycling. This chapter introduces the description of heat-exchangers, problem description, aim and scope of the thesis work.

### 2.1 Background

Engine cooling is an important feature that helps in increasing the efficiency of an automotive engine. During the working of an automobile engine, part of the heat generated by the engine is converted into power and some of it is released through the exhaust system. The remaining waste heat is rejected from the engine into the atmosphere by the cooling system.

In automobile engines, radiators are used as heat exchangers for cooling the engine. A typical radiator can be seen in *Figure 2.1*. A cooling system consists of series of channels in the engine block that allows the coolant liquid to flow through them, a radiator, a pump and a thermostat.



*Figure 2.1. A typical radiator.*

A cooling system works by sending a liquid coolant through passages in the engine block and heads. During this phase, heat from the engine is absorbed by the coolant. This hot fluid goes to the radiator through a rubber hose. As

the coolant flows through the thin tubes present in the radiator, it is cooled by the air stream. Once the fluid is cooled, the same cycle is repeated. The pump does the job of keeping the fluid moving throughout the system.

At TitanX, Radiators are manufactured according to the customer's specifications and are tested to see if the desired specifications have been achieved or not. The Quality assurance of a product that is manufactured is given the utmost priority in any industry. It's a way of preventing unwanted mistakes in manufacturing process and avoiding any problems when delivering solutions to the customers.

## 2.2 Problem description

The analysis of the data such as temperatures, pressures and flows, obtained from the validation tests is quite cumbersome task. A data file is produced in the logging system at the end of every day of the test. A Wöhler test generally takes one to two months depending upon the flow of the coolant. There is no coordinated approach in TitanX to analyze the data of the whole test. It is most important to observe the quality of the test and to check if the test has been performed at the targeted level.

It is also important to accurately predict the durability of the radiators which depends on the Basquin's coefficient. There is no validation for the Basquin's coefficient considered in TitanX which is equal to 5.

## 2.3 Aim and objectives

The main aim of the thesis work is as follows:

- Develop a tool in MATLAB that could import measured data from tests in a structured way, visualize time histories of the test parameters such as temperature, pressure and flow and perform cycle counting method to produce Level Crossing curves (LCC) for all parameters.
- Investigation of Basquin's coefficient from strain measurements and Wöhler tests and determination of an optimal value.

The objectives of the work are:

- Literature study regarding the strain gauges.
- Installation of strain gauges at critical positions that are found from the previous tests and perform strain measurements for different flows.
- Wöhler testing: Thermal cycling for three different flows.
- Data importing, development of an algorithm for Level Crossing cycle counting and development of tool (GUI) in MATLAB.
- Analysis of data from Wöhler tests using the tool developed in MATLAB to see if the test has been performed at a targeted level.
- Determination of an optimal value of Basquin's coefficient from strain measurements and Wöhler test.
- Construction of S-N curve.

### **Scope of the work**

- The tool developed can be extended to the other validation tests that are performed like that of TitanX and can visualize LCCs to check the quality of the test.
- The optimal value of Basquin's coefficient determined helps in the accurate prediction of the damage of the radiators.

## **2.4 Research Questions**

Can a tool be developed in MATLAB that could import measured data from the tests, perform Level Crossing cycle counting and produce LCCs to see if the test has been performed at a targeted level?

Is the Basquin's coefficient considered now, an optimal value?

## **2.5 Delimitations**

The Wöhler testing has been performed only on pure radiators, standing freely in the test bench to minimize the effect from surroundings. Hence, the Basquin's coefficient obtained is valid for pure radiators but not for those mounted in a whole module.

## **2.6 Disposition**

This thesis report starts with the introduction of radiators, problem description, related work, literature survey and the studied system. It then moves on to the overview of the method, the experimentation process, the development of the tool and the investigation of Basquin's coefficient. The next chapters contain the results, discussions and conclusions that are drawn from the work. The report ends with the future works and the references.

# 3 Related work

## 3.1 Literature study

The literature on cycle counting methods, strain gauges and their functionality has been carried out.

### 3.1.1 Strain gauges

A strain gauge is a device which is used for the measurements of surface strains. It can also be defined as an electric sensor which measures the strain.

Carbon gauges are the first type of strain gauges that were used. They were used by Charles Kearns who measured the surface strains to improve the blade design of propeller blades. Carbon composition resistors were used in these strain gauges. Resistance stability with time and temperature is low in these type of strain gauges. These gauges were restricted to measurement of dynamic strains because of the lack the resistance stability [1].

Bonded wire strain gauges are extensively used after the carbon gauges as they produced smaller resistance changes than the carbon strain gauges. In this strain gauges a small diameter wire made of any electrical resistant materials is attached to a structure to find the surface strains. Because of the small resistance changes, these strain gauges have an advantage over carbon gauges when measuring the static and dynamic strains.

Based on the same operating principle as the bonded wire strain gauges, foil strain gauges were introduced. Foil strain gauges are the most extensively used strain gauges in the present market. One of the main reasons of its extensive usage is because of its ability to be used at very high temperatures. Foil gauges are produced by etching or cutting the desired gage pattern into a thin sheet of metal foil of the appropriate alloy [1]. A typical foil strain gauge is shown in *Figure 3.1*. The gauge nomenclature of a foil strain gauge is shown in *Figure 3.2*.

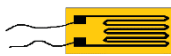


Figure 3.1. A foil strain gauge.

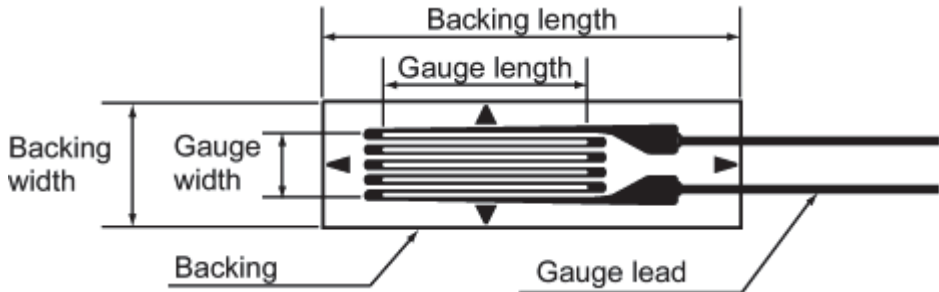


Figure 3.2. Gauge nomenclature [2].

The foil strain gauges have more advantages compared to the bonded wire strain gauges. The difference in them is because:

- The exposed surface of the foil conductor is greater for the same cross-sectional area resulting in a complete strain transmission to the grid.
- Because of a better thermal path from the foil conductor to the substrate, they can operate at higher power levels.
- Manufacturing process of the foil strain gauges is carried out by a photoetching process where as the wire gauges are manufactured by hand.

### Strain gauge bonding

Adhesives are used to attach the strain gauge to the structure that is analysed. Adhesives must be compatible with the gauge, the specimen material and the requirements of the test. The adhesive used must be chosen carefully since the operating characteristics are not the same in different situations. Due to this several adhesive systems are developed by the manufacturers. There are several types of adhesives such as epoxy adhesives, cyanoacrylate adhesives, thermoplastic adhesives, thermosetting adhesives, phenolic adhesives, polyimide adhesives etc.

## Gauge factor

The gauge factor of a strain gauge is defined as the ratio of the resistance change in the gage to the unstrained gauge resistance and the engineering strain. The gauge factor is obtained from the manufacturer.

$$GF = \frac{\Delta R / R_0}{\varepsilon} \quad (3.1)$$

Where,  $\Delta R$  is the change in resistance in the gauge.

$R_0$  Is the unstrained gauge resistance and  $\varepsilon$  is the strain.

## Measurement of resistance

A strain gauge is a resistor. Its resistance changes as the strain changes. As the gauge wire is of very small diameter, the change in resistance is effectively small. So, it is difficult to measure these small changes. And, the device that is being used to measure the strain gauge's resistance will have the resistance of its own. To overcome this problem a Wheatstone bridge is used. It is an electrical circuit which is used to measure an unknown resistance. It works on balancing the legs of a bridge circuit. The unknown resistance is placed in one leg of the circuit. A typical Wheatstone bridge is shown in *Figure 3.3*.

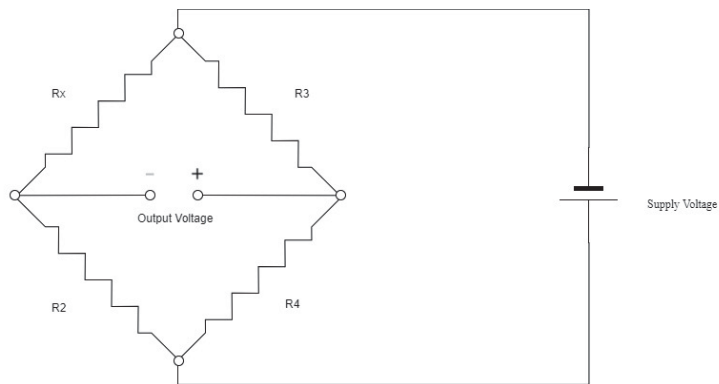


*Figure 3.3. Wheatstone bridge.*

In *Figure 3.3*, the unknown resistance  $R_x$  can be found out if resistances of other resistors, supply voltage and the output voltage are known. If the output voltage is zero volts, the value of resistance  $R_x$  can be found out using the following relation:

$$\frac{R_x}{R_2} = \frac{R_3}{R_4} \rightarrow R_x = \frac{R_3}{R_4} * R_2 \quad (3.2)$$

If all the values of resistors are equal, then the circuit is known as a perfectly balanced bridge. However, during the working operation as the resistance of the strain gauge changes, the output voltage 2 will not be zero. Hence, to measure the resistance, the output voltage and the strain value must be known. To calculate this output voltage, a voltmeter is used.

For calibration, a shunt resistor may be added to the bridge. A Wheatstone bridge with a shunt resistor can be seen in *Figure 3.4*.  $R_s$  is the resistance of the Shunt resistor.

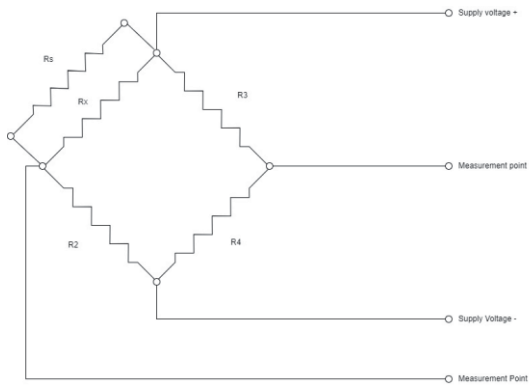


*Figure 3.4. Wheatstone bridge with Shunt resistor.*

To relate the measured voltage to the resistance change, the voltage between the two measuring points is calculated with the shunt resistor across  $R_x$  first and is also calculated without the shunt resistor.

After calculating the resistance change, it is related to strain using the gauge factor.

### Strain gauge configurations

The most common strain gauge configurations are the Quarter bridge circuit, the half bridge circuit and the full bridge circuit.

In a quarter-bridge circuit, one of the resistor is replaced by a strain gauge. The ratio of the two arms of the circuit (on the other side) are set to equal. So, the bridge is balanced when there is no usage of strain gauge. When the strain gauge is either compressed or under tension, the bridge is unbalanced because of the change in the resistance. This results a change in the output voltage leading to the measurement of strain. There are two configurations in quarter-bridge circuit, the two-wire circuit and three wire circuit.

The typical two wires and three wire quarter bridge circuits can be seen in *Figure 3.5 & Figure 3.6*.

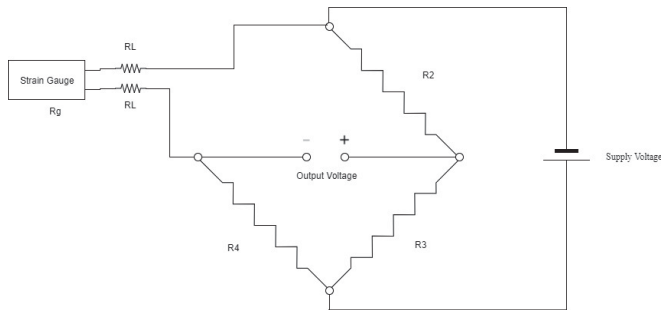


*Figure 3.5. Two-wire quarter-bridge circuit.*

The wire resistance plays an important role in the operation of the circuit. The lead wires that connect the strain gauge to the circuit also have a resistance ( $R_L$ ). If this resistance is negligible then the bridge remains balanced. But the lead wires have some internal resistance. So, the gauge arm resistance becomes the sum of the gauge resistance and twice the lead wire resistance. The main problems of this type of circuit are that it influences the sensitivity, it causes an initial imbalance. Another major problem arises when the temperature of the lead wires changes during the strain measurement process. This may lead to a change in the resistance of the lead wires. To overcome these problems, a third wire is added to the circuit. It is shown in *Figure 3.6*. The two-wire quarter bridge circuit is mainly used for dynamic strain measurements.

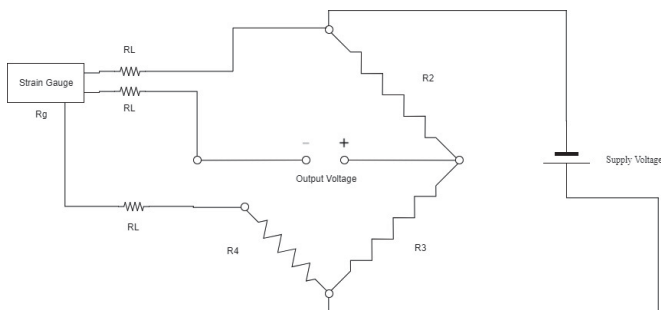


*Figure 3.6. Three-wire quarter-bridge circuit.*

In the three-wire quarter bridge, the first lead wire is in series with the gauge. The second wire is in series with the resistor ( $R_4$ - dummy resistor). The third wire is a voltage sensing wire. The advantages of this configuration is that it

offers greater measurement sensitivity, the effect of change in temperature in lead wires is resolved and it offers intrinsic bridge balance.

Half-bridge circuit consists of two strain gauges in place of two resistors. In this type, both the strain gauges can be placed on the test piece. These strain gauges are placed perpendicular to each other which results in more responsive measurement. Because of this arrangement, the effects of change in temperature are nullified. This is the main advantage of this type of configuration. A typical half-bridge circuit can be seen in *Figure 3.7*.

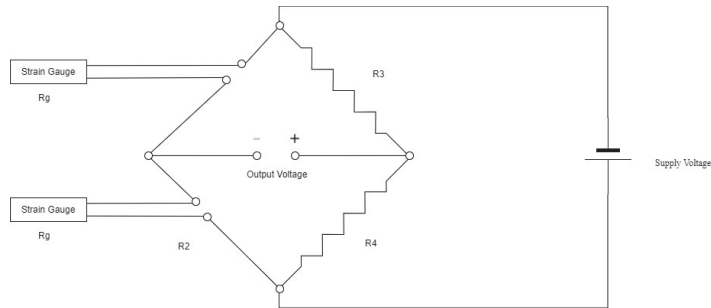


*Figure 3.7. Half-bridge circuit.*

Full-bridge circuit consists of four strain gauges. All the arms of the circuit are replaced by strain gauges. This type of configuration offers the highest degree of accuracy. Another main advantage of this configuration is that the output voltage is proportional to the applied force. A typical full-bridge circuit can be seen in *Figure 3.8*.

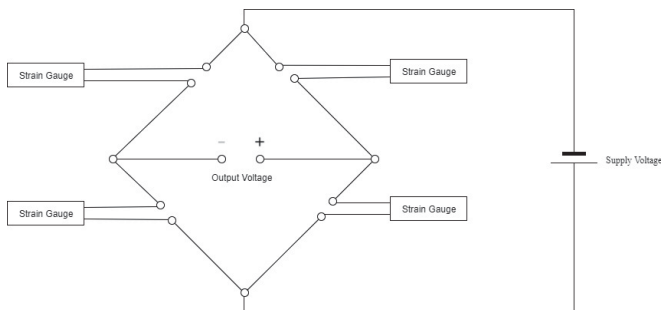


*Figure 3.8. Full-bridge circuit.*

The main disadvantage of the half-bridge and full-bridge circuits is that it is difficult to install complementary pairs of strain gauges to the test piece. This leads to frequent usage of quarter-bridge circuit in strain measurement systems.

### 3.1.2 Cycle counting methods

Cycle counting methods are applied on load signals. Load signals in this context refers to any physical quantity that is changing over time. Some typical loads may be temperatures, flows, pressure etc., most load signals can be described as a function varying over time. The measurement process is in such a way that the samples are recorded at a specified sampling rate. This set of data may be referred as a time history or load history. Cycle counting methods reduce the data from the load histories in different ways which have their own advantages [3].

The cycle counting methods are divided into two categories:

- Amplitude-based methods

In amplitude-based methods, the turning points of the signal are taken into consideration [3]. They do not depend on the rate of the load signal. They are the fundamental methods for the durability prediction.

- Frequency-based methods

In frequency-based methods, the rate of the load signal is taken into consideration. They are mostly used for system load analysis.

However, each method has its own specialty and can reduce the load signal in a different way in different scenarios.

Amplitude-based methods: As mentioned, the amplitude based methods only focus on the local maxima and minima of the signal, which are the turning points of the signal. The counting methods are again classified into cycle counting methods and level crossing methods. The cycle counting methods counts the number of cycles in the load signal using an algorithm.

#### Cycle counting

Cycle counting methods count the number of cycles in the load signal. There are different methods for cycle counting, each having its own algorithm. There are different methods of cycle counting such as range-pair cycle counting, rainflow cycle counting, markov counting etc.

Before starting the cycle counting procedure, pre-processing needs to be performed on the signal [3].

i) Pre-processing:

In this step, unnecessary information is filtered from the load signal. This is done in the following way.

a) Determination of turning points

In this step, the turning points of the signal are found out. This step reduces the data points in the signal to a very large extent. The intermediate points in the signal are neglected. This step does not affect the durability estimation as the intermediate points do not affect the durability in a large extent.

b) Discretization

In this step, the load range in the signal is divided into a number of levels (bins) and each load value is identified with the level it belongs to. The discretized points may be less than the turning points of the signal as two consecutive turning points are considered in the same bin. Normally, the signal is discretized with a bin size of 128.

ii) Cycle counting

A cycle is counted if the load value of the signal goes from a maximum value to a minimum value and again a maximum value (or vice versa). If the signal goes from maximum to minimum (or vice versa) it is known as a half cycle. Two half cycles constitute to one full cycle of the signal.

a) Markov cycle counting [3]

The Markov cycle counting method uses a simple algorithm for counting the cycles in the signal. In this method, the local minima and local maxima are paired into a set. The half cycles are defined as the local minima and local maxima are paired.

For a discretized load signal, the markov cycle counting results are stored in a matrix. In the matrix, the number of transitions from bin  $i$  to bin  $j$  are stored. The whole number of transitions in the markov matrix are also stored in the matrix.

b) Level crossing counting [4]

The level crossing counting procedure counts the number of times the load crosses a level. In this method, the up-crossings and the down-crossings are counted each time the load crosses a load level. The level crossing count can be obtained from Markov matrix. From the Markov matrix, looking at the load levels, the up-crossing and down-crossings are obtained. The obtained results are plotted in a graph to obtain the level crossing curve. This plot gives an overview of the distribution of the signal across the range of the signal.

## 4 Studied system

The function of a radiator is to cool the engine by sending the coolant through passages in the engine block. The coolant absorbs heat from the engine and is sent into the radiators that flows into the tubes where the heat is absorbed thereby cooling the coolant. The fins in between the tubes adds more efficiency to the heat absorption. The radiator studied is shown in *Figure 4.1*, which consists of 88 tubes, 2 rows thick (named as engine side and grill side). The tubes are counted from left to right when observed from the engine side and the numbering can be seen in *Appendix A*.



*Figure 4.1. Studied Radiator.*

A thermal cycling test bench is used for the Wöhler testing. In the test bench, the hot cycle temperature and the cold cycle temperature, the pressure and the flow rate are defined. The test bench can handle temperatures up to 105°C ( $\pm 5^\circ\text{C}$ ) in the hot cycle and -10°C ( $\pm 5^\circ\text{C}$ ) in the cold cycle. It can handle a maximum pressure of 150kPa ( $\pm 15\text{kPa}$ ) and a maximum flow of 200 l/min. The test bench simulates cold start conditions. The coolant consists of 50% glycol mixture. Thermocouples are used to measure the temperatures at inlet and outlet. The pressure is measured at inlet and flow is measured at outlet using a pressure gauge and flow gauge respectively. A logging system records the data from the test at a specified sampling rate. The thermal cycling test bench used is shown in *Figure 4.2*.



*Figure 4.2. Thermal cycling Test Bench.*

## 4.1 Material data and Material Model

The inlet and outlet tanks of the radiator are made from a mixture of plastic. The tubes and the fins of the radiator are made of Aluminum. The properties of Aluminum are shown in *Table 4.1*.

*Table 4.1. Material properties of Aluminum.*

Property	Value in SI units
Density	2700 Kg/m <sup>3</sup>
Modulus of Elasticity	69 GPa

## 5 Overview of the Method

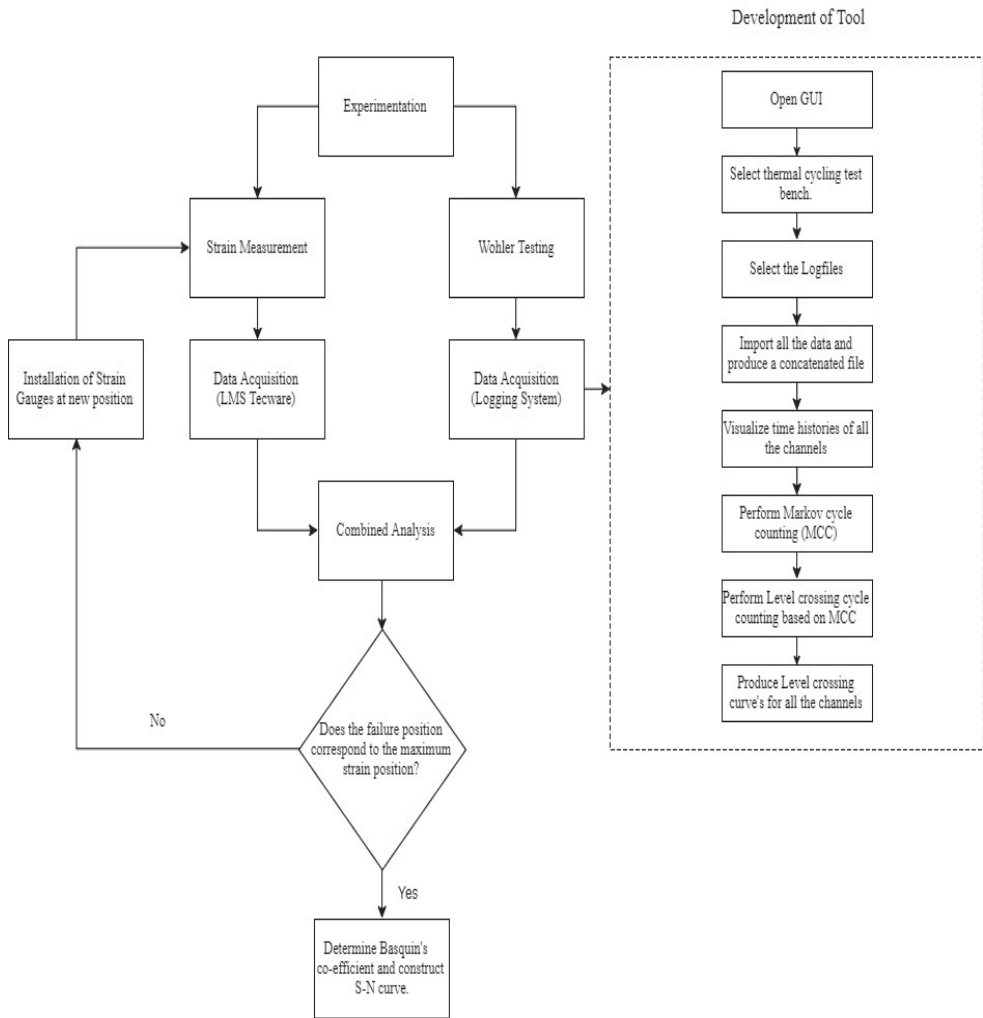


Figure 5.1. Method overview.

# 6 Experimentation process

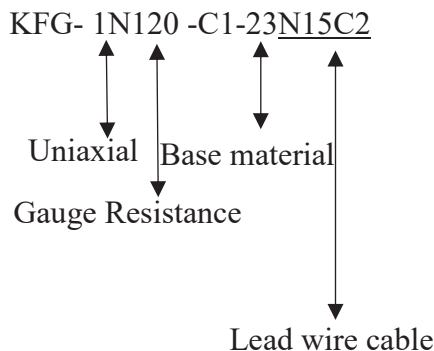
## 6.1 Strain Measurements

The experimentation process starts with measurement of strain on the radiator for different flows. For this purpose, strain gauges are equipped on the radiator. The selection of strain gauge is the first important step in this process.

The requirements that the selected strain gauges should meet are:

- The size of the strain gauge should be small.
- The backing material must be the same as that of the material of the test piece. This is to facilitate the same rate of thermal expansion as that of the test piece.
- Uniaxial strain gauge, as the strains are measured in a single direction

Based on the above required properties, Kyowa strain gauges are used for the measurement of strains on the radiator. The model number of the strain gauges used is KFG-1N120-C1-23N15C2. The first half part of the model number gives us description about the pattern, the gauge resistance and the backing material whereas the second part of the model number describes the type of lead wire used and its length.



From the above serial number of the strain gauge, it can be deduced that a uniaxial strain gauge with a gauge resistance of  $120\Omega$  is used. The base

material of the strain gauge is aluminum and the type of lead wire is Polyester-coated 2-wire copper cable of a length 15cm.

The gauge dimensions are shown in *Table 6.1*.

*Table 6.1. Gauge dimensions.*

Grid(mm)		Base(mm)	
Length	Width	Length	Width
1	0.65	4.2	1.4

The strain gauge has a gauge factor (GF) of 2.1 and a gauge resistance ( $R_0$ ) of  $120\Omega$ . The lead wires of length 15cm are pre-attached to the gauge. A picture of the stain gauge used is shown in the *Figure 6.1*.

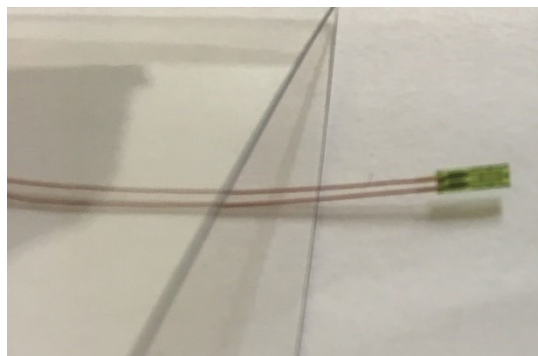


*Figure 6.1. Kyowa Strain gauge.*

The standardized distance for the placing the strain gauges is 7mm from the header-tube joint to the center of the gauge. The strain gauges are placed on the flat side of the tubes and on the tube noose. This is because the flat side has the highest strain levels. The positioning of strain gauges is based on the previous failure positions of the radiator. Looking at the data from the previous tests, the radiator always fails at the outer most tubes. Taking this as a reference, strain gauges are placed on the outermost tubes of the radiator.

The positions at which strain gauges are installed are shown in *Table 6.2*.

*Table 6.2. Position of strain gauges.*

Position of strain gauges								
Engine side (Tube)	Inlet	Outlet	Outlet	Outlet	Outlet	Outlet	Outlet	Outlet
	88 (left and right)	1 (left and right)	2 (left and right)	87 (left and right)	88 (left)	88 (right- 3,7,11 mm)	40 (right)	40 (tube noose)
Front side (Tube)	Outlet							
	40(Tube noose)							

The pictures of strain gauges installed on the radiator are shown in *Figure 6.2.*

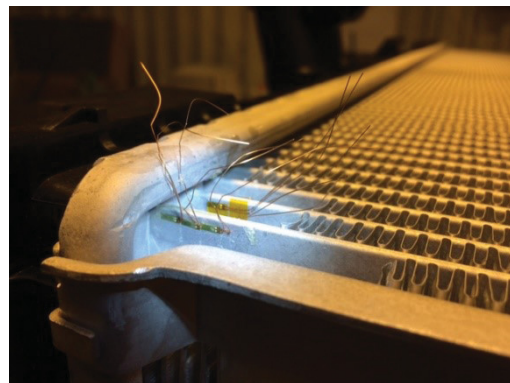


*Figure 6.2. Strain gauges installed on Radiator.*

The adhesive used to attach the strain gauges to the test piece is HBM-X280. It is a two component epoxy resin adhesive. The set-up is now placed in an oven at 95°C for a duration of 1 hour. For accurate measurement of strains there must be no gap between the material and the strain gauge. To achieve this, for the strain gauges on the tube noose, silicon rubber is placed on the strain gauges and heavy weights are placed on the rubber, while for the strain gauges on flat side of the tubes, a special clamping device is used. This process removes any gap between the material and the strain gauges. For the final step in the installation of strain gauges, protective coating (HBM-SG250) is applied on strain gauges.

A quarter bridge 3 wire circuit is used for the measurement of the change in resistance. This type of circuit is used because it offers high measurement sensitivity. The strain gauges mounted on the radiator along with the solder terminal and the bridge circuit can be seen in *Figure 6.3*. The strain gauges are then connected to the data acquisition unit, LMS Scadas recorder. It can directly be connected to a personal computer for calibration and analysis purposes.

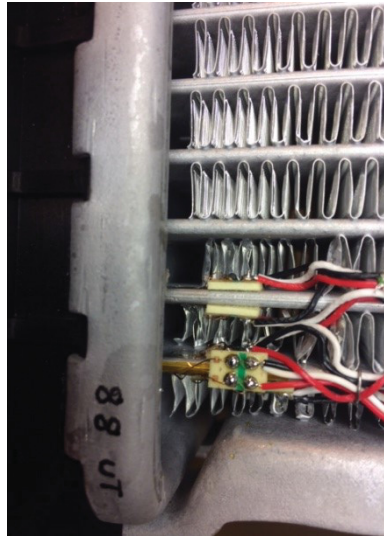


*Figure 6.3. Strain gauges with the solder terminal and bridge circuit.*

The next step is to mount the radiator in the test bench. Air is removed from the radiator before starting the test. This is done by filling the radiator with the coolant while having a small pipe in the top of the radiator to remove air. When there are no bubbles observed, it is concluded that there is no air in the radiator. The resistance of the strain gauge after mounting and at the connector are also measured. The Scadas recorder is connected to a computer which has LMS Test Lab v14.8. The first step is to perform channel set up in the software. In this step, the details of the strain gauges used, information about the position of strain gauges are specified. An excitation voltage of 2V is used for the bridge. A bandwidth of 32Hz is used and a sampling frequency of 64Hz is used. The details of channel set-up analysis can be seen in *Table 6.3*.

Table 6.3. Channel set-up analysis.

Point	Quantity	Position	Inlet/outlet	Tube no	Name	Strain						
						Gauge supplier	Gauge factor	Gauge resistance	Batch	Distance ditch-center strain gauge/mm	Resistance after mounting	Resistance at the connector
1	Strain	Tube	Inlet	88	EngIn_88_left	Kyowa KFG-1N120_C1_23N15C2	2.10	120.0 Y649F	7	119.5	120.2	
2	Strain	Tube	Inlet	88	EngIn_88_right	Kyowa KFG-1N120_C1_23N15C2	2.10	120.0 Y649F	7	119.4	120.3	
3	Strain	Tube	Outlet	1	EngOut_1_left	Kyowa KFG-1N120_C1_23N15C2	2.10	120.0 Y649F	7	119.3	120.2	
4	Strain	Tube	Outlet	1	EngOut_1_right	Kyowa KFG-1N120_C1_23N15C2	2.10	120.0 Y649F	7	119.6	120.4	
5	Strain	Tube	Outlet	2	EngOut_2_left	Kyowa KFG-1N120_C1_23N15C2	2.10	120.0 Y649F	7	119.5	120.3	
6	Strain	Tube	Outlet	2	EngOut_2_right	Kyowa KFG-1N120_C1_23N15C2	2.10	120.0 Y649F	7	119.3	120.2	
7	Strain	Tube	Outlet	87	EngOut_87_left	Kyowa KFG-1N120_C1_23N15C2	2.10	120.0 Y649F	7	119.5	122.6	
8	Strain	Tube	Outlet	87	EngOut_87_right	Kyowa KFG-1N120_C1_23N15C2	2.10	120.0 Y649F	7	119.4	122.6	
9	Strain	Tube	Outlet	88	EngOut_88_left	Kyowa KFG-1N120_C1_23N15C2	2.10	120.0 Y649F	7	119.3	122.5	
10	Strain	Tube	Outlet	88	EngOut_88_right_1	Kyowa KFG-1N120_C1_23N15C2	2.10	120.0 Y649F	7	119.5	122.6	
11	Strain	Tube	Outlet	88	EngOut_88_right_2	Kyowa KFG-1N120_C1_23N15C2	2.10	120.0 Y649F	3	119.5	122.6	
12	Strain	Tube	Outlet	88	EngOut_88_right_3	Kyowa KFG-1N120_C1_23N15C2	2.10	120.0 Y649F	11	119.5	122.7	
13	Strain	Tube	Outlet	40	EngOut_40_left	Kyowa KFG-1N120_C1_23N15C2	2.10	120.0 Y649F	7	119.6	122.8	
14	Strain	Tube	Outlet	40	EngOut_40_right	Kyowa KFG-1N120_C1_23N15C2	2.10	120.0 Y649F	7	119.6	122.6	
15	Strain	Tube	Outlet	40	FroOut_40	Kyowa KFG-1N120_C1_23N15C2	2.10	120.0 Y649F	7	119.2	122.3	
16	Strain	Tube	Outlet	40	FroOut_40	Kyowa KFG-1N120_C1_23N15C2	2.10	120.0 Y649F	7	119.4	122.3	
17	Temp	None	-	-	None							
18	Temp	None	-	-	None							
19	Flow	None	-	-	Flow @outlet							
20	Pressure	Inlet	-	-	Pressure @inlet							

The second step is to perform calibration in the software. This is the most important step and it is performed before starting the measurements. In the calibration step, the offset for pressure and flow are calculated. In the offset calculation, the mA (4mA to 20mA) signal of the test bench is converted into voltage signal (2V to 10V), which is used by LMS Test Lab.

The third step is to perform bridge nulling and shunt calibration. Bridge nulling sets all the values of the bridge to zero. After this, shunt calibration is performed to establish a relation between the millivolt signal and strain. The shunt resistor has a resistance of  $80\text{k}\Omega$ . A strain gauge with a shunt resistance is shown in Figure 6.4. In Figure 6.4,  $R_s$  is the shunt resistance and  $R_x$  is the gauge resistance.

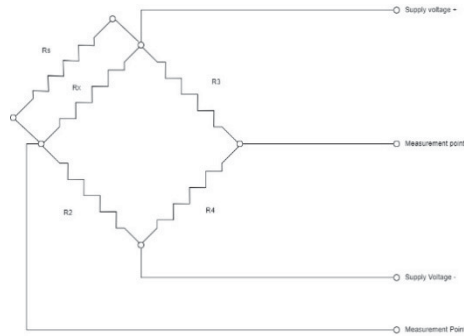


Figure 6.4. Bridge with Shunt resistance.

The relation between the strain and the shunt resistance is as follows:

$$\varepsilon = \frac{R_1}{GF * (R_1 * R_s)} * 10^6 \quad (6.1)$$

where  $R_1$  is the gauge resistance and  $R_s$  is the shunt resistance.

The strain measurements are performed on the radiator for the following flow rates: 50 l/min, 70 l/min, 85 l/min, 100 l/min and 120 l/min. The breakaways

are cut in the beginning to facilitate uniform distribution of strain. As the test is performed in a thermal cycling test bench, the temperature of the coolant varies from hot cycle to cold cycle. The flow rate and the pressure are set to the specified value. But it is observed that the flow rate changes to some extent from the prescribed value during the hot and cold cycles of the test. This is because of different density of the coolant at different temperatures. The pressure of the coolant also varies because of this reason.

The test specifications are as follows:

- Inlet temperature during hot cycle: 95°C ( $\pm 3^\circ\text{C}$ )
- Inlet temperature during cold cycle: -10°C ( $\pm 3^\circ\text{C}$ )
- Coolant flow: 50 l/min, 70 l/min, 85 l/min, 100 l/min and 120 l/min.
- Pressure (relative): 1 bar ( $\pm 0.2\text{bar}$ )

For each flow rate, the strain measurements are made for up to 10 cycles. The strain measurements are saved in an asci format. The results obtained from the strain measurements are discussed in the Chapter 6.3.1.

## 6.2 Wöhler Testing

For Wöhler testing, three tests are performed with different internal coolant flows until failure where two radiators are used for each test. The test specifications are same as that of strain measurements and the flow rates are 50 l/min, 70 l/min and 85 l/min. The set-up of Wöhler testing can be observed in *Figure 6.5*.



*Figure 6.5. Two radiators mounted in the test bench.*

Objects 1&2 are tested until failure for a flow of 85 l/min, 3&4 for a flow of 50 l/min, 5&6 for a flow of 70 l/min. The breakaways are cut before starting the test which can be observed in *Figure 6.6*.



*Figure 6.6. Radiator with cut breakaways.*

There is no automatic failure detection for small leakage. It is determined manually by observing the radiator. In case of heavy leakage, a test bench stopping system is available which activates when the coolant falls in the plate below the radiator. The test data is acquired using a National instrument logging system. The logging system stores a text file for each day of the test. The number of cycles can be seen in the test bench control panel. The results from the Wöhler testing will be discussed in Chapter 6.3.2.

## 6.3 Results from experimentation

### 6.3.1 Strain measurements

The results from strain measurements are obtained as data files which contain strain values ( $\mu\epsilon$ ) at every position on the radiator wherever the strain gauges are installed. LMS Tecware is used for analyzing the data. For each flow, the data is considered for 10 cycles such that the flow rate is constant for all the cycles. Maximum strain values are considered for each flow to compare strains between different positions for a given flow rate which can be observed in *Table 6.4*.

*Table 6.4. Maximum strain range.*

Flow (l/min)	F50 ( $\mu\epsilon$ )	F70 ( $\mu\epsilon$ )	F85 ( $\mu\epsilon$ )	F100 ( $\mu\epsilon$ )	F105 ( $\mu\epsilon$ )	F120 ( $\mu\epsilon$ )	F50_new ( $\mu\epsilon$ )	F85_new ( $\mu\epsilon$ )
Position								
<b>EngIn_88_left</b>	422.5	375.9	379.9	420.2	390.3	382.4	498.3	468.5
<b>EngIn_88_right</b>	344.8	388.2	425.7	452.4	462.2	489.0	333.6	443.9
<b>EngOut_1_left</b>	672.4	795.8	757.9	762.8	741.8	599.5	622.0	740.1
<b>EngOut_1_right</b>	1329	1496	1549	1523	1535	1389	1319	1502
<b>EngOut_2_left</b>	539.2	616.8	664.3	714.7	709.4	745.6	541.6	660.5
<b>EngOut_2_right</b>	639.1	833.7	815.6	762.9	800.2	562.6	588.8	770.8
<b>EngOut_87_left</b>	362.0	391.2	384.4	380.8	353.2	351.6	371.0	372.4
<b>EngOut_87_right</b>	543.3	599.5	637.6	684.8	695.1	747.0	519.9	621.0
<b>EngOut_88_left</b>	908.9	935.0	909.8	906.8	882.6	874.5	915.0	892.5
<b>EngOut_88_right_7mm</b>	298.9	253.1	215.5	220.4	195.5	203.3	301.5	216.4
<b>EngOut_88_right_3mm</b>	314.1	298.8	311.5	304.8	323.8	323.8	341.2	335.5
<b>EngOut_88_right_11mm</b>	302.8	273.8	250.9	259.2	227.7	238.2	309.2	247.7
<b>EngOut_40_right</b>							234.5	264.5
<b>EngOut_40</b>							171.7	274.8
<b>FrOut_40</b>							341.9	335.9
<b>Pressure_inlet</b>	50.8	34.9	36.3	54.1	42.3	57.2	48.8	44.1
<b>Flow_outlet</b>	32.7	22.0	16.3	20.5	23.7	30.6	29.5	26.2
<b>Temp_inlet</b>	102.8	104.2	106.6	106.6	107.4	106.7	103.5	106.7
<b>Temp_outlet</b>	94.7	99.0	102.4	102.9	104.0	103.8	96.2	101.6

The maximum strain values for all the positions are plotted as bar graphs as presented in *Figure 6.7*.

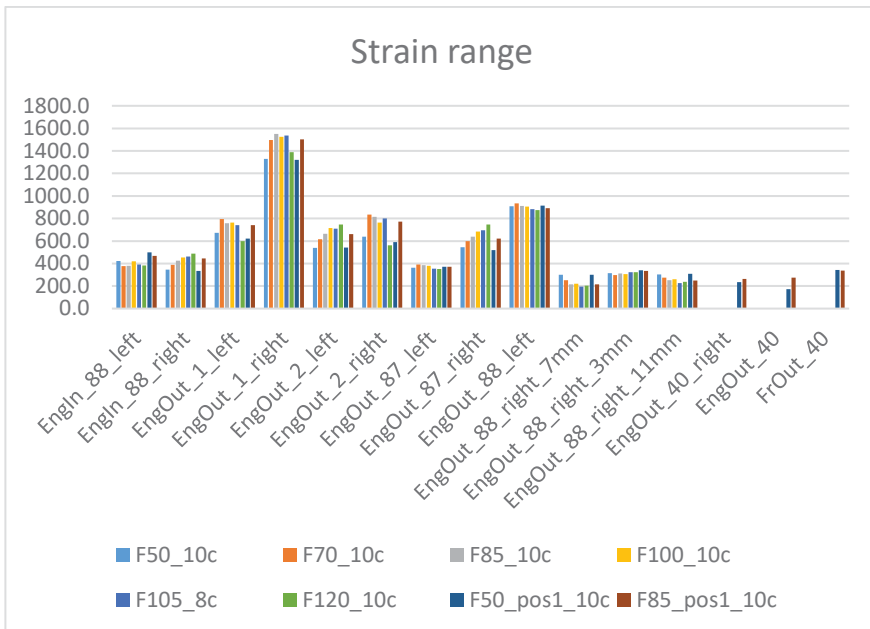


*Figure 6.7. Strain Range.*

It can be observed that tube 1 on Engine outlet side to the right of the tube has the highest strain of  $1329\mu\epsilon$ . Measurements at tube 40 on the Engine side and the grill side are performed only for two flow rates, 50 l/min and 85 l/min. From the strain data, the expected failure position from Wöhler test would be the first tube on Engine outlet side.

### 6.3.2 Wöhler testing

As mentioned earlier, Wöhler test is carried out until failure. The test is stopped when any leakage is detected.

a) Flow rate of 85 l/min:

For object 1, leakage is detected after 6675 cycles. The type of failure is Tube-header leakage. The leakage positions are as follows:

- Engine side outlet tube 39,40,43,44 and Front side outlet tube 39, 42. The failure positions can be observed in *Figure 6.8*.



*Figure 6.8. Failure positions of object 1.*

For object 2, leakage is detected after 7380 cycles. The type of failure is Tube-header leakage. The leakage position is as follows:

- Engine side outlet tube 40. The failure position can be observed in *Figure 6.9*.

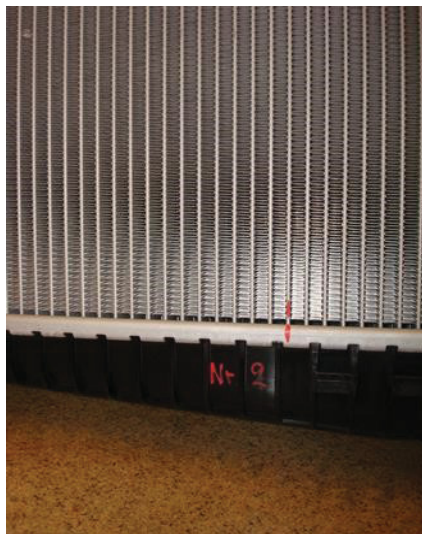


*Figure 6.9. Failure position of object 2.*

b) Flow rate of 50 l/min:

For object 3, leakage is detected after 12240 cycles. The type of failure is Tube-header leakage. The leakage position is as follows:

- Grill side outlet tube 1 (right hand flat side of tube).

For object 4, leakage is detected after 12054 cycles. The type of failure is Tube-header leakage. The leakage position is as follows:

- Grill side outlet tube 1 (right hand flat side of tube). The failure position can be observed in *Figure 6.10*.



*Figure 6.10. Failure position of object 4.*

c) Flow rate of 70 l/min:

For object 5, leakage is detected after 6794 cycles. The type of failure is Tube-header leakage. The leakage position is as follows:

- Grill side outlet tube 39. The failure position can be observed in *Figure 6.11*.



*Figure 6.11. Failure position of object 5.*

For object 6, leakage is detected after 6794 cycles. The type of failure is Tube-header leakage. The leakage position is as follows:

- Engine side outlet tube 49. The failure position can be observed in *Figure 6.12*.

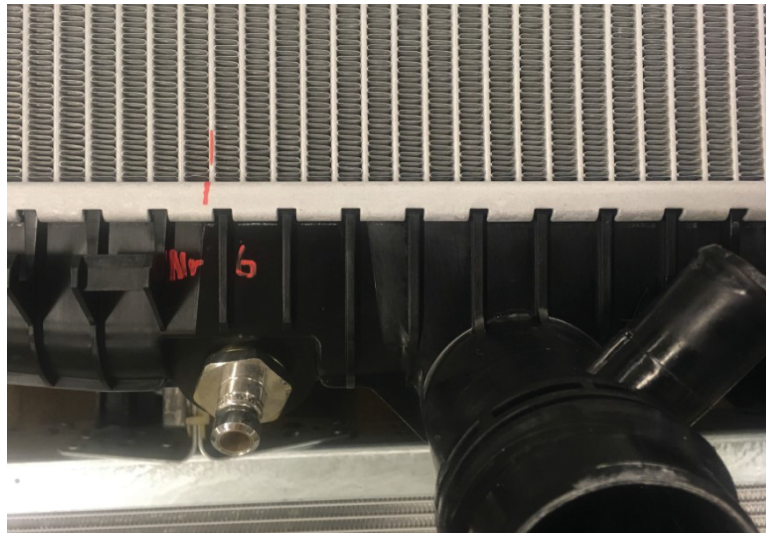


*Figure 6.12. Failure position of object 6.*

The number of cycles to failure for each object can be seen in *Table 6.5*.

*Table 6.5. Cycles to failure of each object.*

Object number	Flow rate (l/min)	Number of cycles	Failure Type
1	85	6675	Tube-header leakage
2	85	7380	Tube-header leakage
3	50	12240	Tube-header leakage
4	50	12054	Tube-header leakage
5	70	6794	Tube-header leakage
6	70	6794	Tube-header leakage

From the strain measurement results, the expected failure position is assumed to be at the tube with the highest strain i.e., Engine side outlet tube 1, but looking at the results from Wöhler test, the failure positions did not correlate with the expected position. Only objects 3&4 fail at the first tube on the grill side outlet. The failure positions of the other objects are almost at the center tubes of the radiator.

To investigate the results, thermographic images of objects 5&6 are produced using an infrared camera, shown in *Figure 6.13 & Figure 6.14*. From the images, it can be observed that there is a temperature lag in the failure position. This is because of clogging in the tubes with the accumulation of dirt.

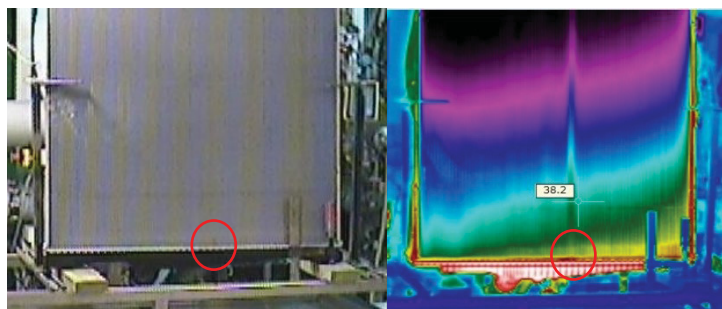


*Figure 6.13. Failure position compared with thermographic image of object 5.*

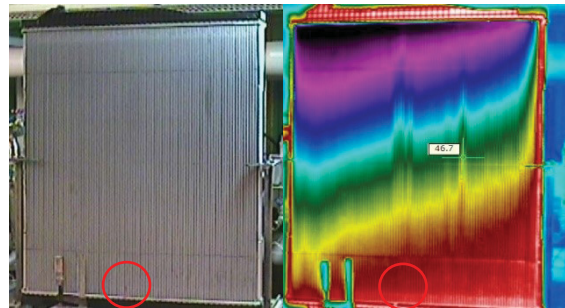


*Figure 6.14. Failure position compared with thermographic image of object 6.*

The positions of failure of the two objects are shown in a red circle. Because of the clogging, the flow rate is reduced at the failure tube which leads to large temperature gradient. Due to this, shear stresses are produced which is the reason failure is observed on the center tubes of the radiator instead of the outermost tubes. The thermo-graphic images for objects 1&2 are not observed, but looking at the failure positions, it is concluded that this is also due to the clogging in the tubes of failure.

# 7 Development of tool

The tool is developed in MATLAB's Graphical User Interface design environment. It allows to create new GUI's or edit the existing GUI's interactively from *fig* files. In this case, a new GUI is created that can import data from all kinds of endurance tests, visualize time histories and produce Level crossing curves for all the parameters in the data.

## 7.1 Data importing

The first step in the development of tool is handling and importing the data from different test benches. The data pattern of each test bench is different because of the variation in number of channels from one test bench to another. Hence, different import functions are created, one for each test bench using the default import tool in MATLAB. This allows to import multiple files from the same test bench.

During the test, the logging system imports data and creates a text file at the end of every day. If a test is carried out for 15 days, 15 data files are produced, one for each day. The data consists of text at the beginning of the file, followed by date, time and the parameters recorded at a sampling frequency. This part of the developed tool handles multiple files from a single test bench, imports data from all the files, ignoring the text at the beginning and produces a concatenated file for the whole test which contains header of the test bench. The header contains the name of the channels, its units, maximum and minimum values and the sampling rate at which the data is recorded.

The examples of two logfiles from a test containing 5 samples each can be seen in *Table 7.1* and *Table 7.2*.

*Table 7.1. Sample data from day 1.*

Thermal cycling test									
Date	Time	Temperature inlet 1	Temperature inlet 2	Temperature outlet 1	Temperature outlet 2	Pressure in 1	Pressure in 2	Flow out 1	Flow out 2
20-3-2017	00:00 :0.0	86.14	91.63	97.3	96.26	48.28	112.4 3	1.54	96.14
20-3-2017	00:00 :2.0	86.04	91.46	97.4	96.23	48.32	112.3 7	1.34	95.79
20-3-2017	00:00 :4.0	85.9	91.44	97.45	96.33	48.79	111.4 3	1.29	96.38
20-3-2017	00:00 :6.0	85.59	91.38	97.5	96.41	49.12	111.8 7	1.45	96.53
20-3-2017	00:00 :8.0	85.53	90.83	97.6	96.42	48.92	112.2 7	1.56	96.32

*Table 7.2. Sample data from day 2.*

Thermal cycling test									
Date	Time	Temperature inlet 1	Temperature inlet 2	Temperature outlet 1	Temperature outlet 2	Pressure in 1	Pressure in 2	Flow out 1	Flow out 2
21-3-2017	00:00 :0.0	83.73	89.84	-6.04	-5	53.64	128.8 1	1.65	84.01
21-3-2017	00:00 :2.0	82.87	89.69	-6.15	-4.87	53.81	128.9	1.72	84.06
21-3-2017	00:00 :4.0	82.76	89.58	-6.33	-4.92	54.3	128.8 3	1.56	84.31
21-3-2017	00:00 :6.0	85.63	89.45	-6.39	-4.88	54.12	130.4 9	1.63	84.19
21-3-2017	00:00 :8.0	85.39	89.37	-6.49	-4.77	53.99	129.9	1.58	84.69

It can be observed from the *Table 7.1* and *Table 7.2* that the sampling frequency at which the data is recorded is 2 seconds.

The data importing part of the developed tool handles these files, imports data and produces a concatenated file which can be seen in *Table 7.3*.

*Table 7.3. Concatenated data of the whole test.*

BEGIN								
CHANNELNAME = ['Temp in LV1','Temp out LV1','Temp in LV2','Temp out LV2','Presure LV1','Pressure LV2','Flow LV1','Flow LV2']								
MINIMUM = [-20,-20,-20,-20,-20,-20,0,0]								
MAXIMUM = [150,150,150,150,400,400,200,200]								
UNIT=['°C','°C','°C','°C','kPa','kPa','l/min','l/min']								
START = 0.0								
RATE = 0.5								
END								
Time	Temperature Inlet 1	Temperature Inlet 2	Temperature Outlet 1	Temperature Outlet 2	Pressure in 1	Pressure in 2	Flow out 1	Flow out 2
0	86.14	91.63	97.3	96.26	48.28	112.43	1.54	96.14
2	86.04	91.46	97.4	96.23	48.32	112.37	1.34	95.79
4	85.9	91.44	97.45	96.33	48.79	111.43	1.29	96.38
6	85.59	91.38	97.5	96.41	49.12	111.87	1.45	96.53
8	85.53	90.83	97.6	96.42	48.92	112.27	1.56	96.32
10	83.73	89.84	-6.04	-5	53.64	128.81	1.65	84.01
12	82.87	89.69	-6.15	-4.87	53.81	128.9	1.72	84.06
14	82.76	89.58	-6.33	-4.92	54.3	128.83	1.56	84.31
16	85.63	89.45	-6.39	-4.88	54.12	130.49	1.63	84.19
18	85.39	89.37	-6.49	-4.77	53.99	129.9	1.58	84.69

In *Table 7.3*, the starting text is known as header, which varies from one test bench to another. The original date and time formats are removed and a new time vector is inserted with the same sampling frequency but is simplified in such a way that it is supported by MATLAB.

## 7.2 Level Crossing Cycle Counting

### 7.2.1 Implementation of Level Crossing Cycle Counting

An algorithm is developed for the Level crossing cycle counting which works based on the Markov cycle counting procedure. Before implementing the method to the real data, synthetic signals are considered whose LCCs are compared to those obtained from LMS Tecware software. The approach of producing LCCs in LMS Tecware is Rainflow cycle counting method.

The following is the algorithm developed for producing LCC.

- Initially, the turning points (peaks and valleys) of the signal are determined using *extrema* function [5].
- The next step is to define the Markov pairs. Starting with the first turning point (TP), the first and second turning point makes one pair, second and third makes another one and it is continued until the last value.
- Once the Markov pairs are defined, the unique matrix of the turning points is considered which is a singleton set of the turning points matrix, arranged in the ascending order.
- The values of the Unique matrix are found out in the first column of Markov matrix, arranged in the order of Unique matrix.
- The respective pairs corresponding to these values are determined in the second column of Markov matrix, named as Unique pairs and arranged in the same order.
- Starting with the first value of Unique matrix, the respective Unique pairs are compared, if they are greater than or equal to the next value of Unique matrix. If so, one cycle is counted for every such positive case.
- Likewise, the procedure is carried out for all the values in the Unique matrix. These gives ‘Upcrossings’.

- The Unique matrix is considered in the reverse order.
- The values in this matrix are found out in the first column of Markov matrix. The respective pairs corresponding to these values are determined in the second column of Markov matrix and are compared, if they are less than or equal to the next value of Unique matrix in reverse order. If so, one cycle is counted for every such positive case.
- Likewise, the procedure is carried out for all the values in the reverse Unique matrix. These gives ‘Downcrossings’.
- The Upcrossings and Downcrossings together gives Level Crossing curve of the signal.

This algorithm is applied for synthetic signals to produce LCC’s and compare them to LCC’s obtained from LMS Tecware.

The following are the two synthetic signals considered.

Signal 1: A sine wave is considered with two different amplitudes, four cycles each as shown in *Figure 7.1*.

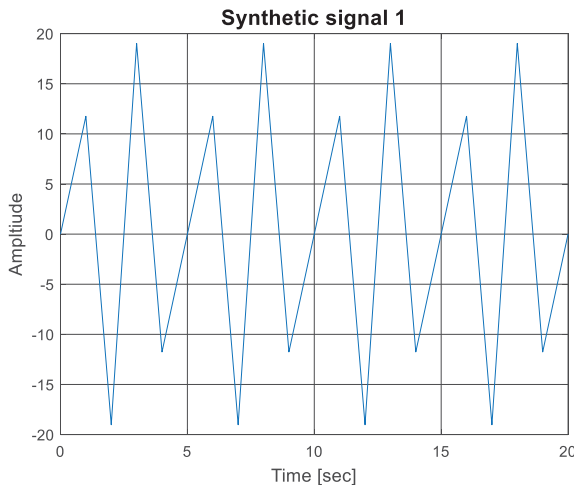


*Figure 7.1. Synthetic signal 1.*

The algorithm developed is applied and the Level crossing curve of the signal is produced as shown in *Figure 7.2*.

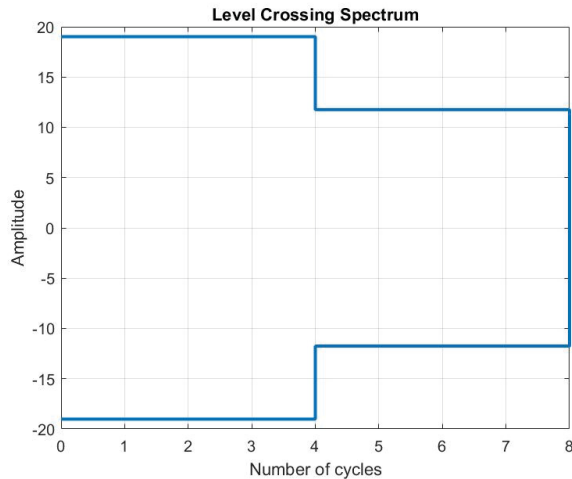


*Figure 7.2. Level crossing curve for synthetic signal I from MATLAB.*

The LCC of the signal is compared to that obtained from LMS Tecware, shown in *Figure 7.3*.

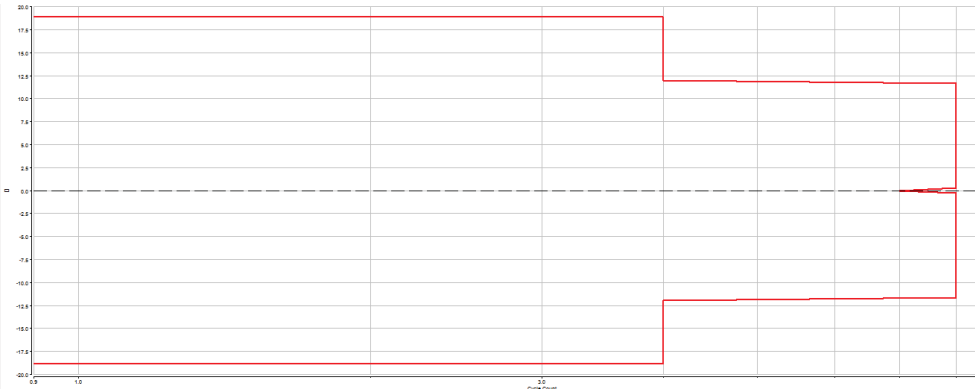


*Figure 7.3. Level crossing curve for synthetic signal I from LMS.*

It can be observed from *Figure 7.2* & *Figure 7.3* that the LCC obtained from the developed algorithm is exactly equal to that obtained from LMS Tecware. Hence, the algorithm is generalized and applied for another signal.

Signal 2: A sine wave is considered with two different amplitudes, ten cycles each as shown in *Figure 7.4*.

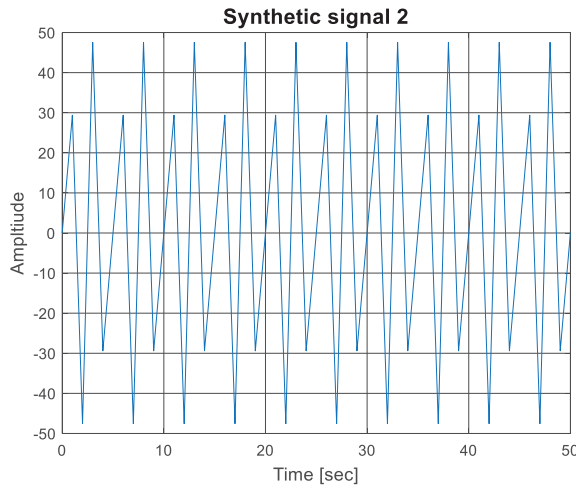


*Figure 7.4. Synthetic signal 2.*

The Level crossing curve of the signal obtained using the developed algorithm is shown in *Figure 7.5*.

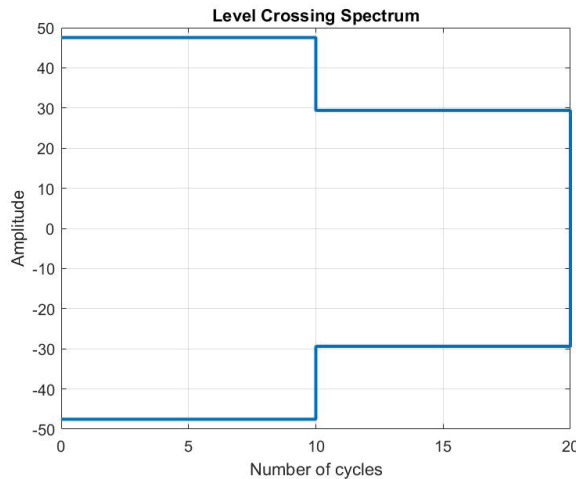


*Figure 7.5. Level crossing curve for synthetic signal 2 from MATLAB.*

The LCC of the signal is compared to that obtained from LMS Tecware, shown in *Figure 7.6*.

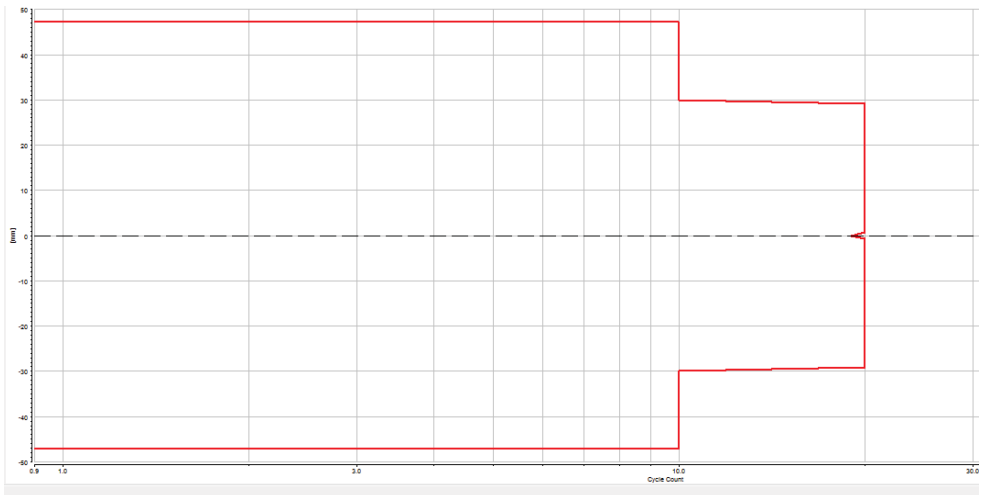


*Figure 7.6. Level crossing curve of synthetic signal 2 from LMS.*

It can be observed from *Figure 7.5 & Figure 7.6* that the LCC of the signal obtained from the generalized algorithm is exactly equal to that computed from LMS Tecware.

### 7.2.2 Real data from test bench

With the algorithm working for synthetic signals, the next step is to apply it to real data obtained from the test bench. The real data obtained from the thermal cycling test bench are shown in *Figure 7.7*, *Figure 7.8* & *Figure 7.9*. From thermal cycling tests, the data of temperature, flow and pressure is obtained.

The time history of temperature for one day of data is shown in *Figure 7.7*.

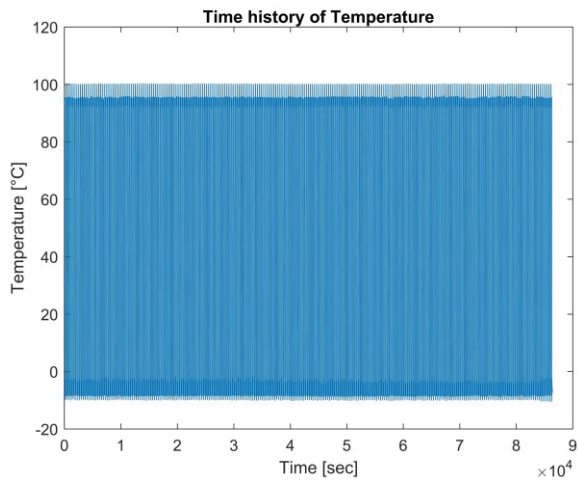


*Figure 7.7. Time history of temperature (1 day).*

The time history of pressure for one day of data is shown in *Figure 7.8*.

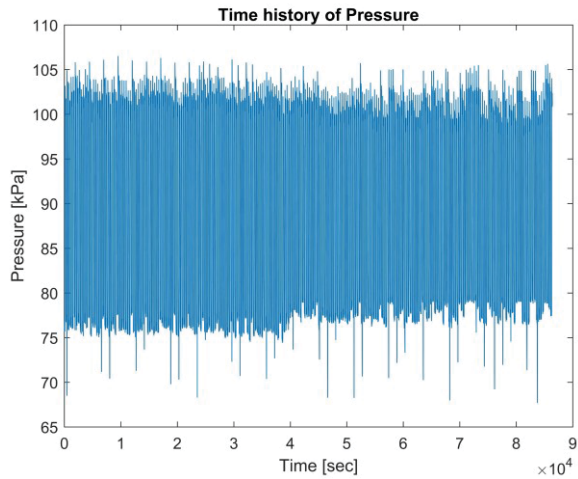


*Figure 7.8. Time history of pressure (1 day).*

The time history of flow for one day of data is shown in *Figure 7.9*.

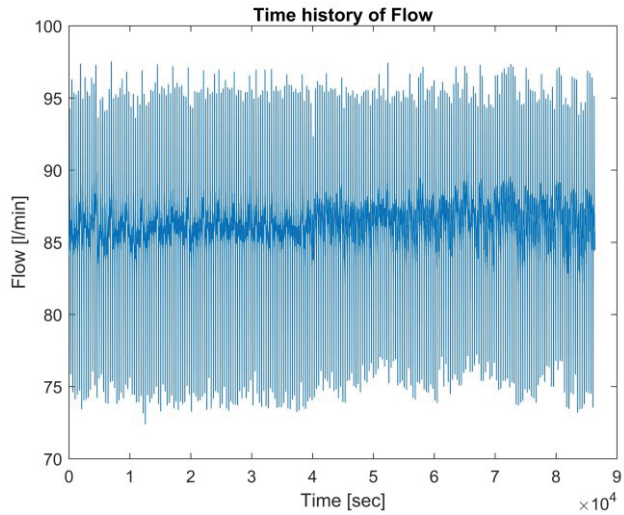


*Figure 7.9. Time history of flow (1 day).*

From these figures, it can be observed that the data obtained from the tests looks like a lump of mass. The same data for a limited number of cycles is shown in *Figure 7.10*, *Figure 7.11* & *Figure 7.12*.

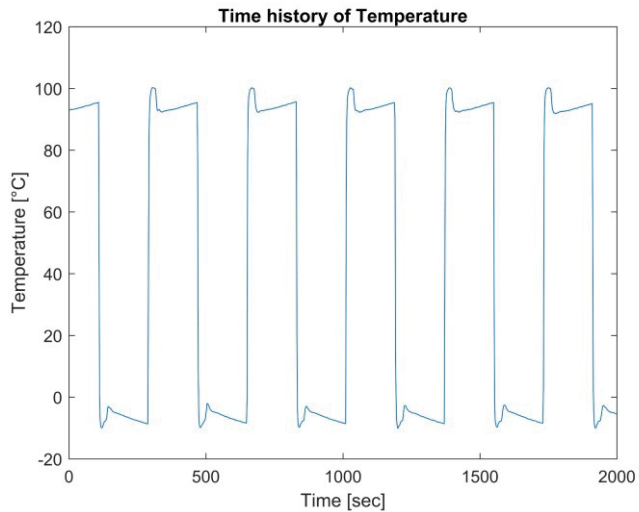


*Figure 7.10. Time history of temperature (5 cycles).*

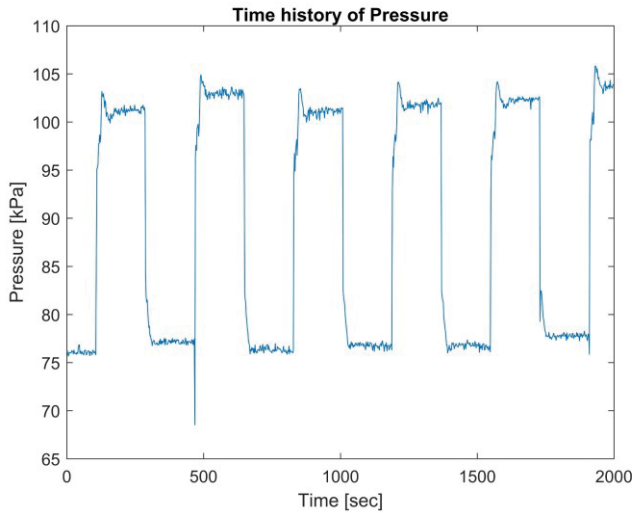


*Figure 7.11. Time history of pressure (5 cycles).*

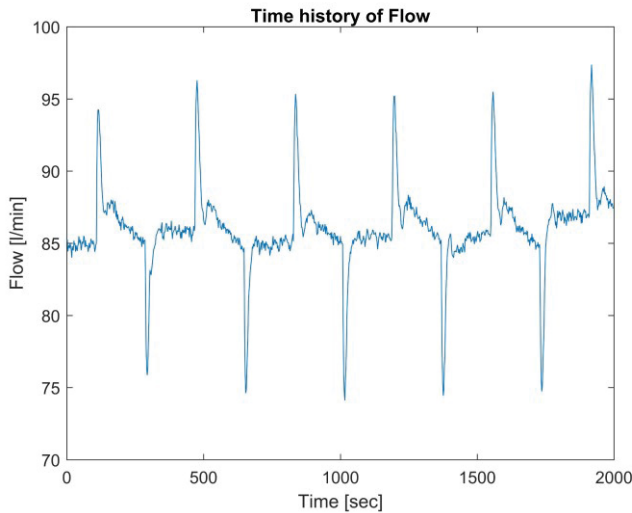


*Figure 7.12. Time history of flow (5 cycles).*

The interpretation of one day data by looking at the time histories is difficult. By looking at a limited number of cycles, there is a better understanding of the process undergoing in the test bench. By producing the level crossing curves of the time histories, a much better understanding of the test data can be obtained.

### 7.2.3 Level Crossing counting for Real data

The generalized algorithm is applied for the real data obtained from the test bench for parameters such as temperature, pressure etc. The level crossing results obtained were observed to be wrong. The algorithm is investigated and observed that the determination of turning points (TPs) doesn't work correctly using *extrema* function in case of complex signals like *Figure 7.10*, *Figure 7.11 & Figure 7.12*.

When these complex signals are compared with the simple synthetic signals, it can be observed that there are a numerous local maxima and minima which makes the *extrema* function difficult to determine the exact global maxima and minima. To overcome this problem, the signal processing toolbox in MATLAB is used to determine the TPs.

The signal processing toolbox in MATLAB works based on a function named as '*findpeaks*'. This is implemented in the algorithm leaving the initial method of determination of peaks using *extrema* function and the level crossing curves are produced for the real data.

The Level crossing curves obtained for the time histories *Figure 7.10*, *Figure 7.11 & Figure 7.12* are shown in *Figure 7.13* *Figure 7.14 & Figure 7.15*.

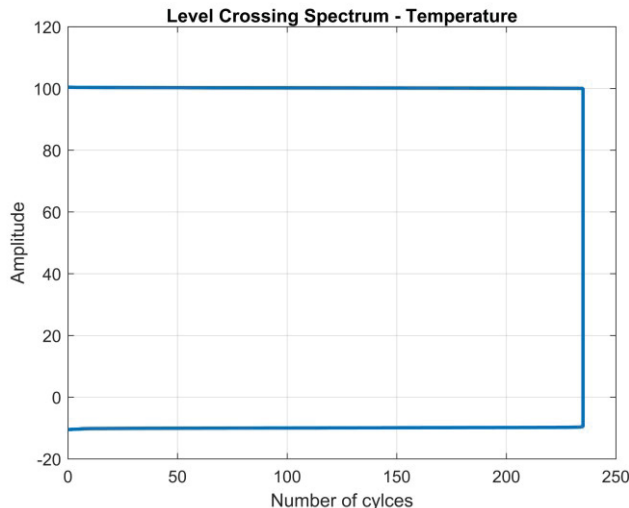


*Figure 7.13. Level crossing curve of Temperature history.*

The level crossing spectrum obtained for pressure history is shown in *Figure 7.14*.

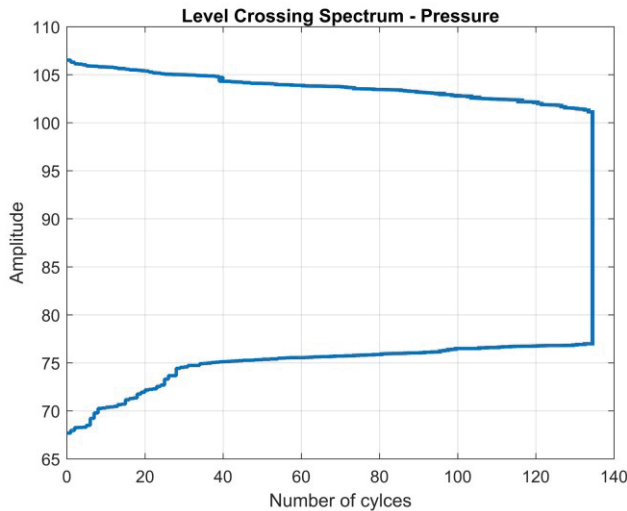


*Figure 7.14. Level crossing curve of Pressure history.*

The level crossing spectrum obtained for flow history is shown in *Figure 7.15*.

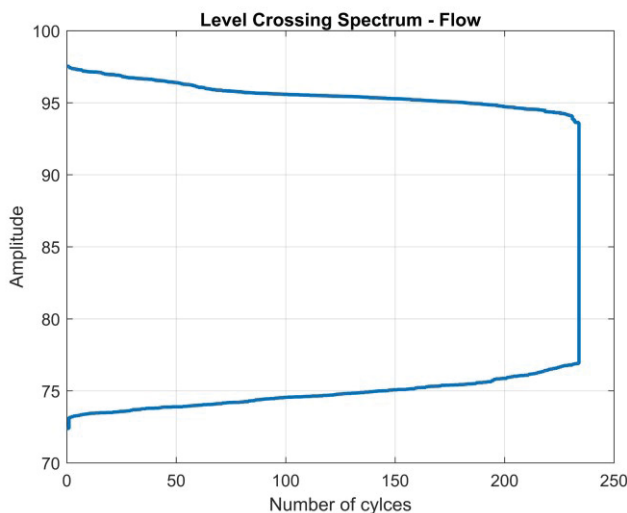


*Figure 7.15. Level crossing curve of Flow history.*

## 7.3 Graphical user interface (GUI)

A graphical user interface is created using MATLAB's graphical user interface design environment. As there are eight different test benches, eight push buttons are created representing each test bench. Different pushbuttons are added for each different test bench which show the time-histories of the respective channel of the test bench. Push buttons are also generated for plotting the level crossing spectrum of each channel of a test bench. The GUI developed can be seen in the *Figure 7.16*.

Using the GUI developed, the level crossing curves are generated for all the objects in Wöhler testing. The results can be seen in Appendix B.

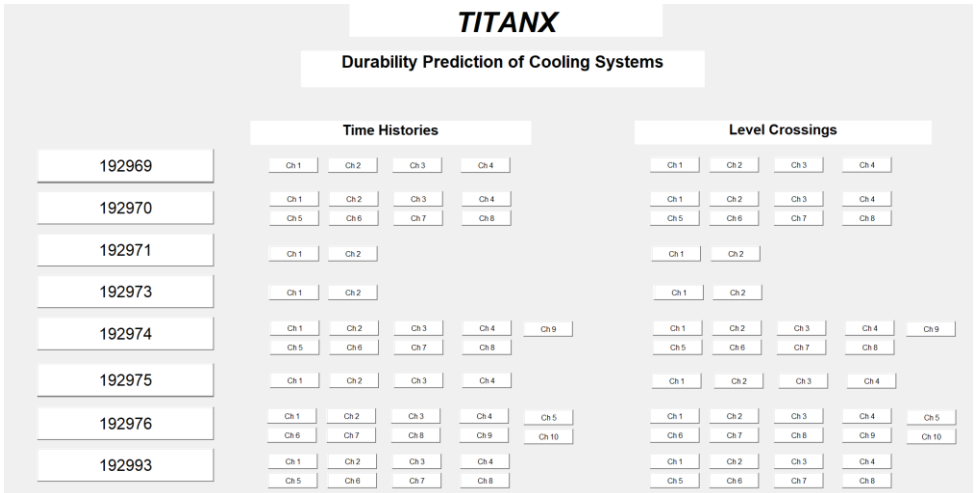


*Figure 7.16. GUI of tool developed.*

## 8 Investigation of Basquin's Coefficient

The Basquin's coefficient is estimated from the results of strain measurements together with those obtained from Wöhler testing. From the Wöhler test, the number of cycles to failure obtained from each flow are considered and from the strain measurements, the highest strain positions are considered. Based on these results, Basquin's coefficient is determined and S-N curve is constructed.

From the results of Wöhler testing, the failure positions of both objects for each flow are as follows: The failure location for a flow of 50 l/min is front side, outlet tube 1, for a flow of 85 l/min the failure positions are on engine side, outlet tubes 39,40,43,44 and front side, outlet tubes 39, 42, for a flow of 70 l/min the failure positions are engine side, outlet tube 49 and grill side, outlet tube 39. From the failure positions and the strain measurements it is observed that strains at all the failure positions are not available. There is not enough data to plot the S-N curve as the strains on all the failure positions are not known. So, an evaluation from the available data is made in this study. The highest stresses induced are calculated from the strain data. The average number of cycles to failure for each flow rate can be seen in *Table 8.1*.

*Table 8.1. Wöhler results.*

S.no	Flow (l/min)	Number of cycles to failure	Average number of cycles
1	85	6675	7028
2	85	7380	
3	50	12240	12147
4	50	12054	
5	70	6794	6794
6	70	6794	

As the highest strains are used for the estimation of Basquin's coefficient, the strains recorded on Engine side (outlet) tube 1 right side are considered for finding the stress values. The above tube is chosen because it has the

highest strain values when the maximum ranges of strain are observed (in *Figure 6.7*).

The stress ( $\sigma$ ) is found out using Hooke's law. The elastic modulus, E of Aluminum is 69 GPa.

$$\sigma = \varepsilon * E \quad (8.1)$$

where  $\varepsilon$  is strain and E is the modulus of elasticity

The values of flow, strain, stress and the number of cycles are shown in *Table 8.2*.

*Table 8.2. Stress and strain values for each flow.*

S.no	Position	Flow (l/min)	Strain (micro strain)	Stress (MPa)	Average number of cycles
1	EngOut_1_right	50	1319.6	91.05	12147
2	EngOut_1_right	70	1496.3	103.245	6794
3	EngOut_1_right	85	1549.2	106.895	7028

The Basquin's coefficient is found out from the Basquin's relation which provides an analytical expression for the S-N curve.

$$N = \alpha * S^{-\beta} \quad (8.2)$$

where  $\alpha$  is a constant depending on material &  $\beta$  is the Basquin's coefficient

Using this analytical expression, the value of  $\beta$  is found out.

The estimation of Basquin's coefficient is done by considering the flows 50 l/min & 85 l/min in one case, 50 l/min & 70 l/min in the other case.

For case (i)

The equation for Basquin's coefficient is given by,

$$N = \alpha * S^{-\beta}$$

For the flow 50 l/min, the equation can be written as,

$$12147 = \alpha * (91.05 * 10^6)^{-\beta}$$

$$\Rightarrow \log(12147) = \log \alpha - \beta * \log(91.05 * 10^6) \rightarrow (1)$$

For the flow 85 l/min, the equation can be written as,

$$7027 = \alpha * (106.9 * 10^6)^{-\beta}$$

$$\Rightarrow \log(7027) = \log\alpha - \beta * \log(106.9 * 10^6) \rightarrow (2)$$

Solving equations (1) and (2),

$$\log(12147) = \log\alpha - \beta * \log(91.05 * 10^6)$$

$$\log(7027) = \log\alpha - \beta * \log(106.9 * 10^6)$$

$$\log\left(\frac{12147}{7027}\right) = \beta * \log\left(\frac{106.9 * 10^6}{91.05 * 10^6}\right)$$

$$0.238 = \beta * 0.069$$

$$\beta = \frac{0.238}{0.069} \cong 3.4$$

$$\beta \cong 3.4$$

For case (ii)

The equation for Basquin's coefficient is given by,

$$N = \alpha * S^{-\beta}$$

For the flow 50 l/min, the equation can be written as,

$$12147 = \alpha * (91.05 * 10^6)^{-\beta}$$

$$\Rightarrow \log(12147) = \log\alpha - \beta * \log(91.05 * 10^6) \rightarrow (1)$$

For the flow 70 l/min, the equation can be written as,

$$6794 = \alpha * (103.25 * 10^6)^{-\beta}$$

$$\Rightarrow \log(6794) = \log\alpha - \beta * \log(103.25 * 10^6) \rightarrow (2)$$

Solving equations (1) and (2),

$$\log(12147) = \log\alpha - \beta * \log(91.05 * 10^6)$$

$$\log(6794) = \log\alpha - \beta * \log(103.25 * 10^6)$$

$$\log\left(\frac{12147}{6794}\right) = \beta * \log\left(\frac{103.25 * 10^6}{91.05 * 10^6}\right)$$

$$0.252 = \beta * 0.055$$

$$\beta = \frac{0.252}{0.055} \cong 4.58$$

$$\beta \cong 4.6$$

The Wöhler curve is plotted for the two cases mentioned above. It consists of the stress on the Y axis and the number of cycles to failure on X axis in logarithmic scale. The obtained curves are shown in *Figure 8.1*.

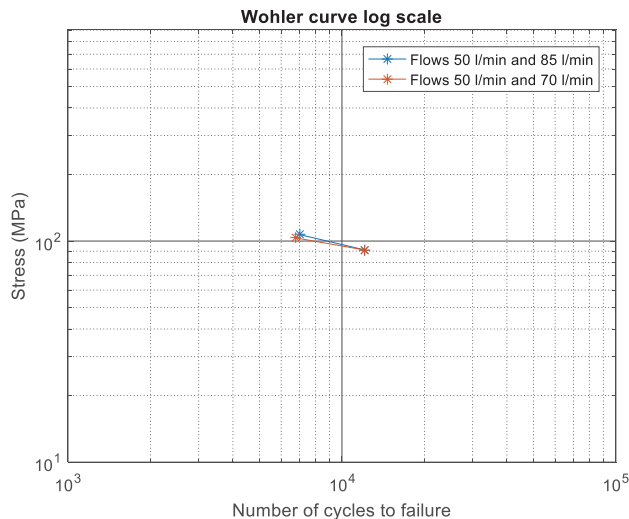


*Figure 8.1. Wöhler curve (log-log scale).*

The Wöhler curve in semi-logarithmic scale is shown in the *Figure 8.2*.

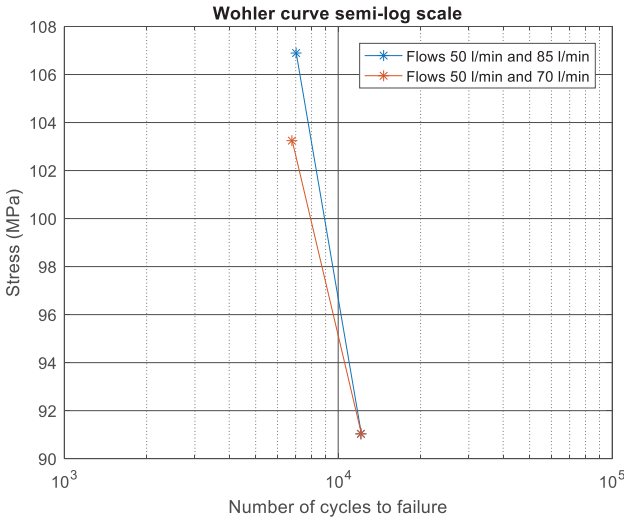


Figure 8.2. Wöhler curve (semi-log scale).

As there was clogging observed in the tubes of objects 5 & 6 there was a premature failure observed in both objects. The failure position of object 3&4 corresponds to failure at expected position (outer tubes). Also, for a flow of 85 l/min, there are no thermographic images. Assuming there is no clogging in objects 1&2, the number of cycles to failure for the flow 70 l/min is calculated from the Basquin's coefficient obtained in case (i).

From case (i), the value of Basquin's coefficient obtained is 3.4.

For the flow 50 l/min, the equation 8.2 can be written as,

$$\begin{aligned}
 12147 &= \alpha * (91.05 * 10^6)^{-\beta} \\
 \Rightarrow \log(12147) &= \log \alpha - 3.4 * \log(91.05 * 10^6) \\
 \log \alpha &= \log(12147) + 3.4 * \log(91.05 * 10^6) \\
 \log \alpha &= 31.14
 \end{aligned}$$

This  $\alpha$  value is used to find the number of cycles to failure for a flow of 70 l/min. As the values of stress,  $\alpha$  and  $\beta$  are known, the actual number of cycles to failure is estimated.

For the flow 70 l/min, the equation 8.2 can be written as,

$$N = \alpha * (S)^{-\beta}$$

$$N = (10)^{31.14} * (103.25 * 10^6)^{-3.4}$$

$$N = 7812$$

Using the number of cycles to failure from the above relation for a flow of 70 l/min, the Basquin's coefficient value for case (ii) is estimated again.

For the flow 50 l/min, the equation can be written as,

$$12147 = \alpha * (91.05 * 10^6)^{-\beta}$$

$$\Rightarrow \log(12147) = \log\alpha - \beta * \log(91.05 * 10^6) \rightarrow (1)$$

For the flow 70 l/min, the equation can be written as,

$$7812 = \alpha * (103.25 * 10^6)^{-\beta}$$

$$\Rightarrow \log(7812) = \log\alpha - \beta * \log(103.25 * 10^6) \rightarrow (2)$$

Solving equations (1) and (2),

$$\log(12147) = \log\alpha - \beta * \log(91.05 * 10^6)$$

$$\log(7812) = \log\alpha - \beta * \log(103.25 * 10^6)$$

$$\log\left(\frac{12147}{7812}\right) = \beta * \log\left(\frac{103.25 * 10^6}{91.05 * 10^6}\right)$$

$$0.191 = \beta * 0.055$$

$$\beta = \frac{0.191}{0.055} \cong 3.47$$

$$\beta \cong 3.5$$

The Basquin's coefficient obtained from case (i) can be considered as approximate or close to the optimal value whereas the result obtained from case (ii) cannot be considered because there were impurities or dirt in the tubes 39-42 for the test of flow 70 l/min. This leads to the clogging of the flow in those tubes and results in premature failure of the specimen without reaching the fatigue limit. When considering the clogging and estimating the actual number of cycles to failure for a flow of 70 l/min, the value of Basquin's coefficient is found out to be 3.5.

## 9 Results

A tool has been developed in MATLAB to check if the test has been performed according to the targeted level. The following are the functions of the tool.

- Different functions are generated for importing the data for different test benches.
- The tool will handle the data files using these functions, imports multiple files and creates a concatenated file.
- The tool shows time histories of all the channels of the data such as temperature, pressure, flow, etc. to see how the parameters are varying with time.
- An algorithm is developed for Level crossing counting that works based on Markov cycle counting method.
- The algorithm produces Level crossing spectra for all the channels of the data which is used for the interpretation of the test.
- The Level crossing spectra also shows the number of cycles of the test. For example, in the *Figure 9.1*, the time history of the temperature is solid mass and is hard to interpret the behavior of the temperature. Whereas, in the *Figure 9.2*, the Level crossing of the time history of the temperature shows that there were 240 load cycles of the temperature ranging from -10 °C to 100 °C.

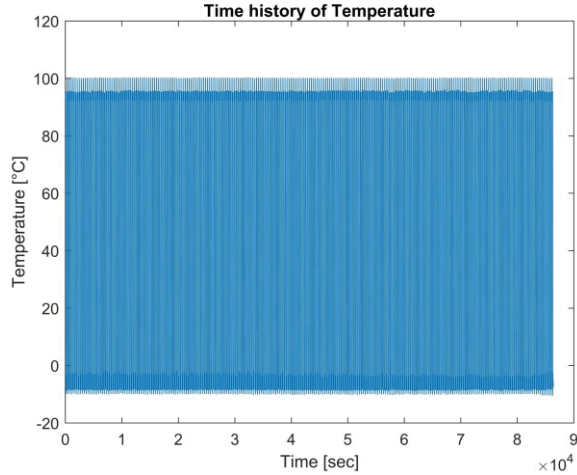


*Figure 9.1. Temperature history of one day data.*

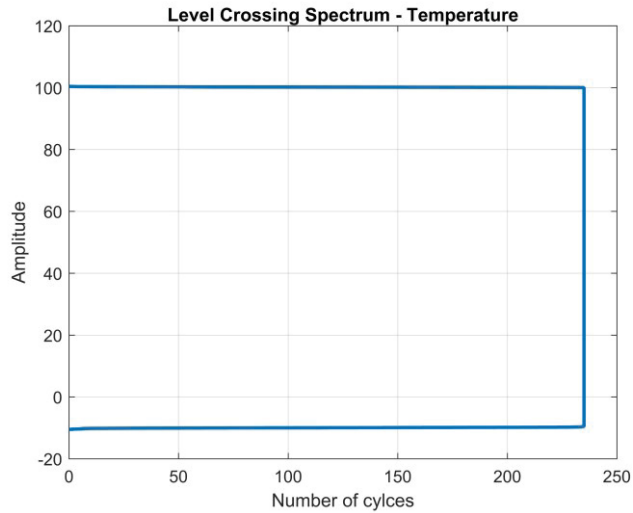


*Figure 9.2. Level crossing spectrum of Temperature data for one day.*

- GUI is generated by integrating all the individual codes for importing the data, algorithms for Markov cycle counting and Level crossing in a structured manner. Different push buttons are implemented for importing the data for different test benches. Every channel of a test bench, two push buttons are implemented for producing time histories and Level crossings.

- Strain measurements are performed for three different flows for 10 cycles. Flows: 50 l/min, 70 l/min and 85 l/min. It was observed that the most fatigue tube is Engine side outlet tube 1 because of the highest strains recorded at that location.
- From the Wöhler tests for the same flows as that of the strain measurements, the failure locations did not coincide with the highest strain position because of the clogging of dirt in the tubes at the failure positions. This leads to the premature failure of the tubes.
- Basquin's coefficient which is determined from the strain measurements and Wöhler testing is found to be 3.4. By finding the actual number of cycles to failure for the flow of 70 l/min, the optimal value of Basquin's coefficient is found to be 3.5

# 10 Summary and Conclusions

In TitanX Engine Cooling, various tests are performed when introducing a new heat-exchanger into the market. The result of the test is a logfile produced in the logging system that contains data of the channels such as temperature, pressure, flow etc. The analysis of the test data is difficult and its interpretation is very important.

The research in the thesis has accomplished this by developing a tool in MATLAB for handling the test data. It performs cycle counting methods: Markov cycle counting and Level crossing counting. Finally, Level crossing spectra are produced for all the parameters in the test data that shows how well a test has been carried out.

The optimal value of basquin's coefficient is determined from the results of strain measurements and Wöhler testing and is found to be 3.5 for a pure radiator.

## 11 Future works

The estimation of Basquin's coefficient is based on the highest strain obtained in the tubes and not on the failure positions. As the strain gauges cannot be placed on each tube of the radiator, a finite element model of the radiator could help to achieve an accurate Basquin's coefficient.

Wöhler testing on the whole radiator module can also be performed to know how the Basquin's coefficient varies when compared to a pure radiator.

To consider the effect of clogging on the overall failure position of the radiator, strain gauges can be installed on the tubes of the radiator at which failure occurs to record the strain range. A theory can be estimated that higher strains will be recorded at the position near failure than the outermost tubes of the radiator.

## 12 References

- [1] R. L. Hannah, S. E. Reed, and Society for experimental mechanics, *Strain gage users' handbook*. Chapman & Hall, 1992.
- [2] “Strain gauge coding system|Strain gauges|Products|Tokyo Sokki Kenkyujo Co., Ltd.” [Online]. Available: [http://www.tml.jp/e/product/strain\\_gauge/gaugetype.html](http://www.tml.jp/e/product/strain_gauge/gaugetype.html). [Accessed: 05-Oct-2017].
- [3] P. Johannesson, M. Speckert, SP Bygg och Mekanik, SP – Sveriges Tekniska Forskningsinstitut, and RISE, *Guide to Load Analysis for Durability in Vehicle Engineering*, 1st ed. Somerset: John Wiley & Sons, Incorporated, 2013.
- [4] Y.-L. Lee, J. Pan, and R. Hathaway, *Fatigue Testing and Analysis*. Butterworth-Heinemann, 2011.
- [5] “extrema.m, extrema2.m - File Exchange - MATLAB Central.” [Online]. Available: <http://se.mathworks.com/matlabcentral/fileexchange/12275-extrema-m-extrema2-m>. [Accessed: 06-Dec-2017].

# 13 Appendix

## A. Numbering of tubes on radiator

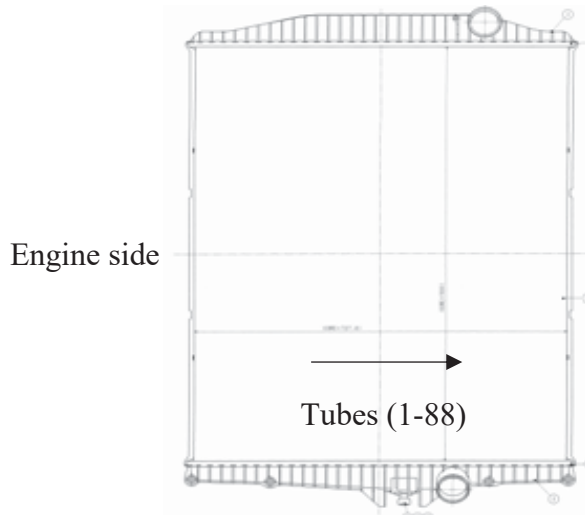
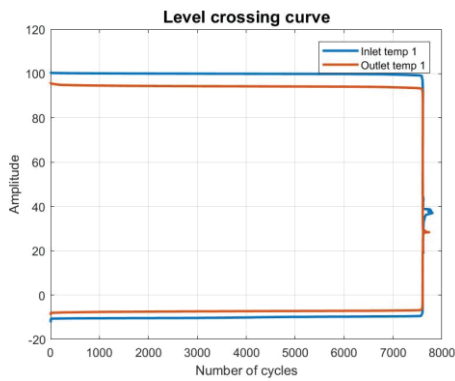


Figure 13.1. Engine side (Tubes 1-88).

## B. Level crossing curves from Wöhler Testing

The level crossing curves obtained from the test data in the thermal cycling test bench for all the six objects.

For Object 1 (Flow-85 l/min):



*Figure 13.2. LCC of Inlet and Outlet Temperature (Object 1).*

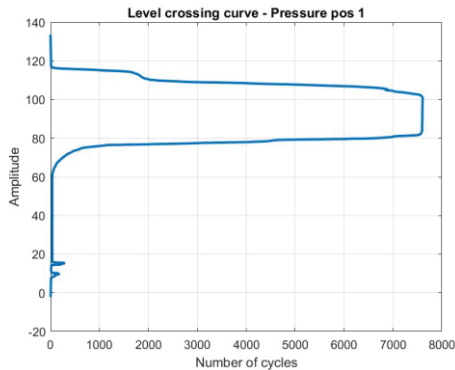


*Figure 13.3. LCC of Pressure (Object 1).*

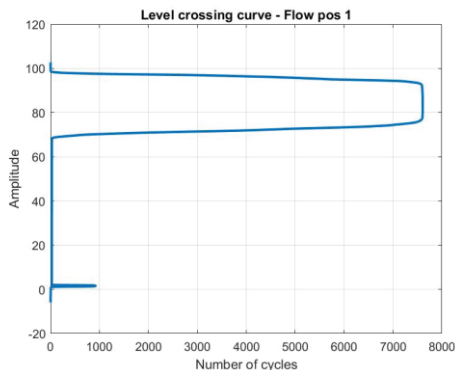


*Figure 13.4. LCC of Flow (Object 1).*

For Object 2 (Flow-85 l/min):

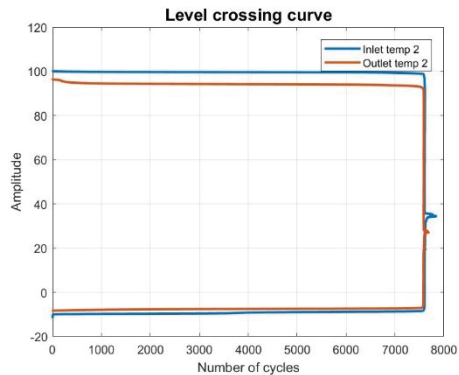


Figure 13.5. LCC of Inlet and Outlet Temperature (Object 2).

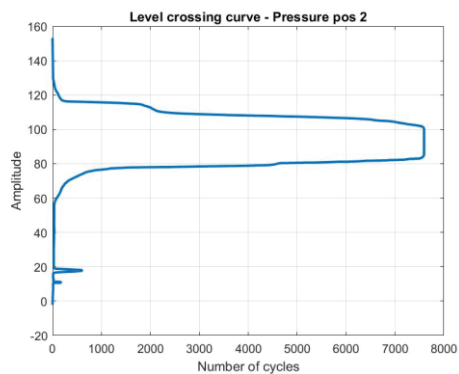


Figure 13.6. LCC of Pressure (Object 2).

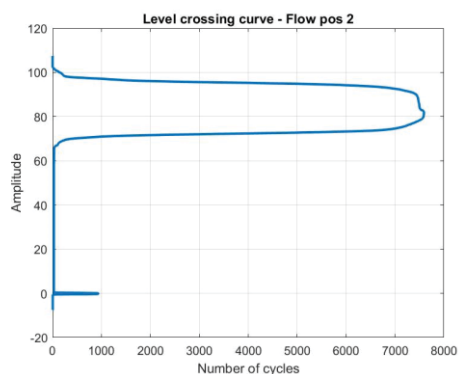


Figure 13.7. LCC of Flow (Object 2).

For Object 3 (Flow-50 l/min):

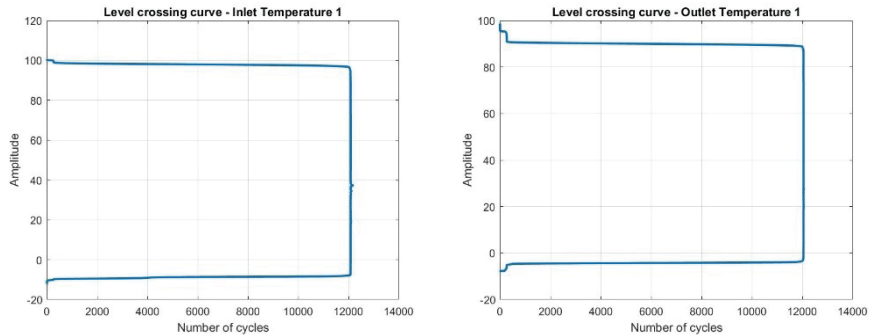


Figure 13.8. LCC of Inlet and Outlet Temperature (Object 3).

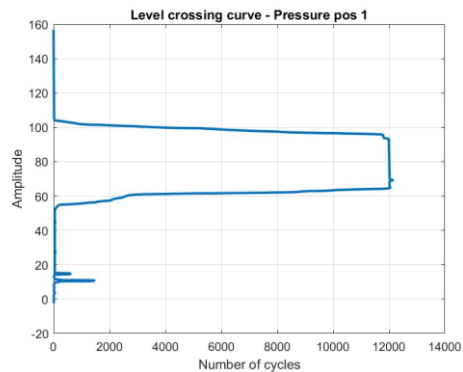


Figure 13.9. LCC of Pressure (Object 3).

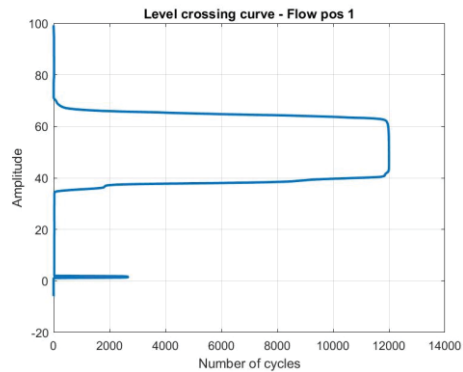


Figure 13.10. LCC of Flow (Object 3).

For Object 4 (Flow-50 l/min):

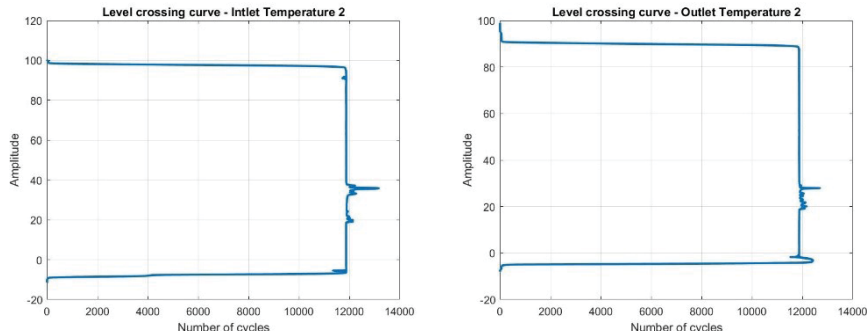


Figure 13.11. LCC of Inlet and Outlet Temperature (Object 4).

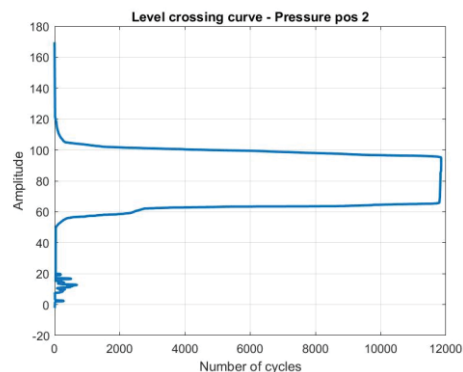


Figure 13.12. LCC of Pressure (Object 4).

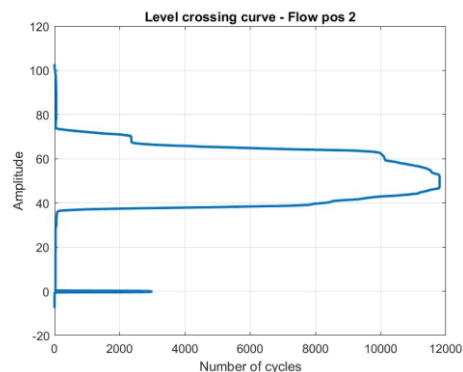


Figure 13.13. LCC of Flow (Object 4).

For Object 5 (Flow-70 l/min):

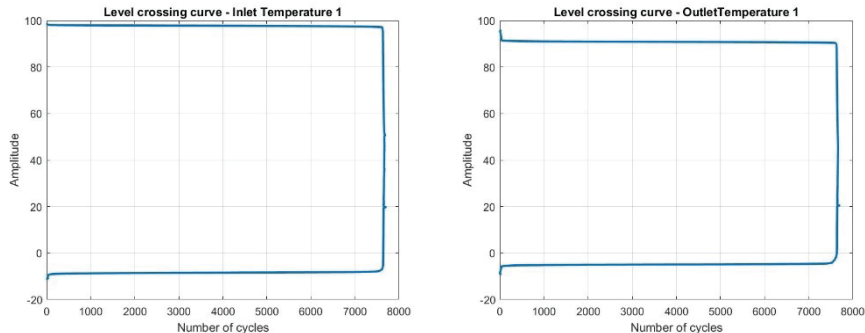


Figure 13.14. LCC of Inlet and Outlet Temperature (Object 5).

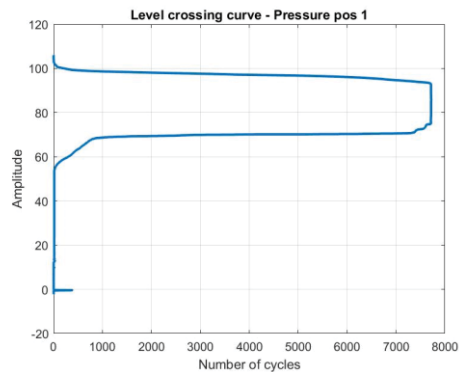


Figure 13.15. LCC of Pressure (Object 5).

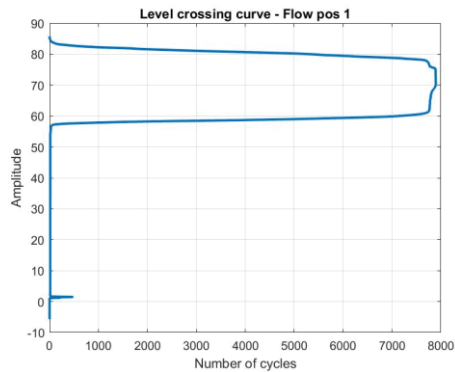


Figure 13.16. LCC of Flow (Object 5).

For Object 6 (Flow-70 l/min):

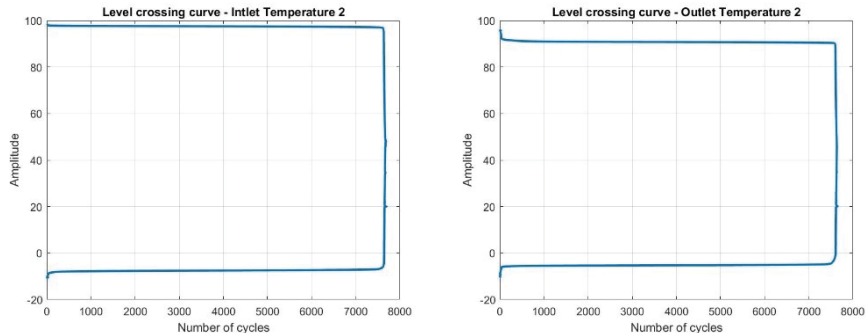


Figure 13.17. LCC of Inlet and Outlet Temperature (Object 6).

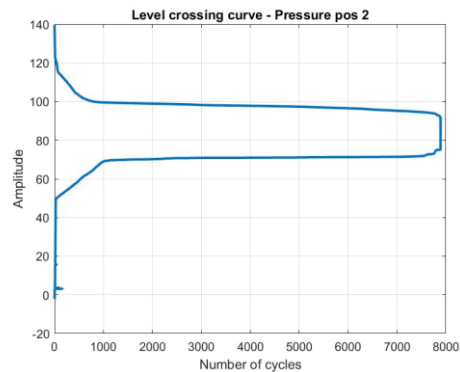


Figure 13.18. LCC of Pressure (Object 6).

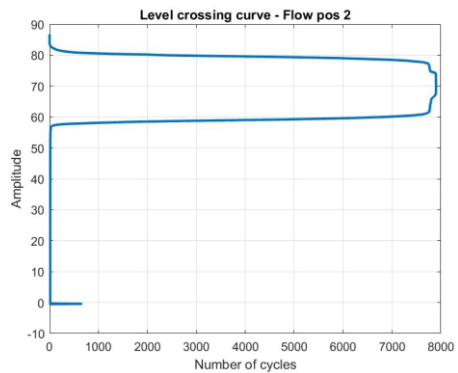


Figure 13.19. LCC of Flow (Object 6).





---

Department of Mechanical Engineering  
Blekinge Institute of Technology  
SE-371 79 Karlskrona, SWEDEN

Telephone: +46 455-38 50 00  
E-mail: [info@bth.se](mailto:info@bth.se)